

**FINAL REPORT**

to

Dr. Mirsajadi Hassan  
Watershed Assessment Section, Division of Water Resources,  
Delaware Natural Resources and Environmental Control (DNREC)  
89 Kings Hwy  
Dover, DE 19901  
Phone: (302) 739-9939  
Email: Hassan.Mirsajadi@state.de.us

**Vertical Profiles of Radioisotopes, Nutrients and Diatoms in Sediment Cores  
from the Tidal Murderkill River Basin:  
A Historical Analysis of Ecological Change and Sediment Accretion**

PCER Report No. 10-XX

By  
Drs. David Velinsky, Christopher Sommerfield<sup>1</sup> and Don Charles  
Patrick Center for Environmental Research  
The Academy of Natural Sciences  
Philadelphia, PA 19103

<sup>1</sup>University of Delaware  
College of Earth, Ocean and Environment  
Lewes, DE

**DRAFT**

May 8, 2010

## TABLE OF CONTENTS

	Page
<b>List of Tables .....</b>	<b>iii</b>
<b>List of Figures.....</b>	<b>iv</b>
<b>Executive Summary .....</b>	<b>v</b>
 <b>A</b>	
<b>Introduction.....</b>	<b>1</b>
A1 Background .....	2
A2 Objectives of Study .....	2
A3 Study Area .....	2
 <b>B</b>	
<b>Field and Laboratory Methods.....</b>	<b>4</b>
B1 Field Sampling .....	4
B2 Laboratory Methods.....	5
B2.1 Radioisotope Measurements and Sedimentation Rates .....	5
B2.2 Total Organic Carbon and Nitrogen .....	8
B2.3 Total Phosphorus.....	8
B2.4 Stable Isotopes of Carbon and Nitrogen .....	8
B2.5 Diatoms .....	9
 <b>C</b>	
<b>Results and Discussion.....</b>	<b>9</b>
C1 Sediment Properties and Sediment Accumulation.....	9
C1.1 Sediment Properties.....	10
C1.2 Accretion and Sediment Accumulation Rates.....	11
C1.3 Radionuclide Inventories and Focusing Factors .....	13
C2 Nutrients/Eutrophication.....	15
C2.1 Sediment Total Carbon, Total Nitrogen and Total Phosphorus .....	15
C2.2 Stable Isotopes of Carbon and Nitrogen .....	16
C2.3 Diatom Analysis and Assemblages .....	18
C3 Historical Analysis.....	22
C3.1 Changes in Nutrients and Diatoms in Murderkill River Cores .....	23
C3.2 Changes in Marsh Ecology .....	25
C3.3 Nitrogen and Phosphorus Accumulation Rates.....	27

## TABLE OF CONTENTS (cont)

	Page
<b>D</b>	
Summary and Conclusions .....	29
<b>E</b>	
Acknowledgments .....	31
<b>F</b>	
References .....	32
<b>G</b>	
Tables .....	40
<b>H</b>	
Figures.....	59
<b>I</b>	
Appendices .....	78
Appendix I: Data Tables and QA Documentation.....	I

## LIST OF TABLES

Table 1: Core Locations and collection dates .....	46
Table 2: Bulk sediment properties and radioisotope data for core MK-1 .....	47
Table 3: Bulk sediment properties and radioisotope data for core MK-2 .....	49
Table 4: Bulk sediment properties and radioisotope data for core MK-3 .....	51
Table 5: Bulk sediment properties and radioisotope data for core MK-4 .....	53
Table 6: Summary data for radioisotope analysis and dating .....	55
Table 7: Concentrations of various parameters for core MK-1 .....	56
Table 8: Concentrations of various parameters for core MK-2 .....	57
Table 9: Concentrations of various parameters for core MK-3 .....	58
Table 10: Concentrations of various parameters for core MK-4 .....	59
Table 11: Diatom metrics for core MK-1 .....	60
Table 12: Diatom metrics for core MK-2 .....	61
Table 13: Diatom metrics for core MK-3 .....	62
Table 14: Diatom metrics for core MK-4 .....	63

## LIST OF FIGURES

Figure 1: Generalized schematic of nitrogen and phosphorus cycling in wetlands.....	65
Figure 2: Study area and core locations.....	66
Figure 3: Tripod/pulley system in the Murderkill River.....	67
Figure 4: Geochronology for core MK-1.....	68
Figure 5: Geochronology for core MK-2.....	68
Figure 6: Geochronology for core MK-3.....	69
Figure 7: Geochronology for core MK-4.....	69
Figure 8: Sediment organic carbon, C/N and sediment phosphorus distribution with depth .....	70
Figure 9: Depth distribution of the isotopic composition sediment N ( $\delta^{15}\text{N}$ ) and C ( $\delta^{13}\text{C}$ ) .....	71
Figure 10: Distribution of diatom indicator species with depth: MK-1.....	72
Figure 11: Distribution of diatom indicator species with depth: MK-2.....	73
Figure 12: Distribution of diatom indicator species with depth: MK-3.....	74
Figure 13: Distribution of diatom indicator species with depth: MK-4.....	75
Figure 14: Diatom metrics .....	76
Figure 15: Relationship between total sediment N and diatom metrics .....	77
Figure 16: Relationship between the accumulation rate of sediment N and P and the diatom metric for eutrophentic species in each core.....	78
Figure 17: Concentrations of total sediment nitrogen (TN) and the nitrogen isotopic composition of TN ( $\delta^{15}\text{N}$ -TN) from 1860 to 2008 .....	79
Figure 18: Concentrations of total sediment phosphorus (TP) and the carbon isotopic composition of total carbon ( $\delta^{13}\text{C}$ -TC) from 1860 to 2008 .....	80
Figure 19: Diatom metric for eutrophentic species from 1860 to 2008.....	81
Figure 20: Nitrogen and phosphorus accumulation with time.....	82

## Executive Summary

This study involved the chemical analysis of five sediment cores taken from the tidal Murderkill River in Kent County, DE. Four were dated using  $^{210}\text{Pb}$  and  $^{137}\text{Cs}$  radiometric methods providing sufficient temporal coverage ( $> 50$  yrs) for detailed chemical analysis. *The main objective was to evaluate historical trends in nutrients (i.e., sediment phosphorus and nitrogen) and to evaluate if a historical record of eutrophication could be derived from analysis of diatom along with other indicators of potential ecosystem change (e.g., stable isotopes of carbon ( $\delta^{13}\text{C-OM}$ ) and nitrogen, ( $\delta^{15}\text{N-TN}$ )).*

**(To be completed once report is reviewed)**

## A) Introduction

### A1: Background

Nutrients, trace metals and organic contaminants in water are derived from many sources. Natural sources of metals include the weathering products of soils which are then transported in the dissolved or particulate phases. Anthropogenic sources of metals and organic contaminants are introduced to the water via atmospheric deposition, industrial discharges (e.g., mining, metal processing, manufacturing), municipal discharges (waste water treatment), and stormwater runoff of contaminated parcels. Many of these same sources are also noted for discharges of nitrogen and phosphorus; especially waste water treatment facilities and agricultural runoff (via surface runoff and indirectly through groundwater flows). Due to the particle-reactive nature of most trace metals, phosphorus, and organic compounds, sediments are potential repositories for contaminants and, under certain conditions, can be used to provide a historical record of pollution (Simpson et al., 1983; Orson et al., 1990; 1992; Valette-Silver, 1993; Hornberger et al., 1999; Cooper and Brush, 1993; Church et al., 2006; Velinsky et al., 2007; Hartzell et al., 2010, and others). With minimal diagenetic remobilization, biological mixing, and hydraulic processes, the sediment column can reflect the chronological deposition/inputs of most contaminants, but with some caveats for both nitrogen and phosphorus which can undergo substantial diagenetic re-mobilization.

Phosphorus is transported to the oceans from rivers and estuaries and up to 90% is in a particulate form (Meybeck, 1982; Froelich et al., 1982; Lebo, 1991; Follmi, 1996; Litke, 1999; Jordan et al., 2008). Once bound phosphorus is buried, it has the potential to be recycled back into the water column depending on many factors (Froelich et al., 1982; Boynton et al., 1995; Jordan et al., 2008; **Figure 1**). In some sub-tidal environments, only a small portion of the buried phosphorus (e.g., 5 to 30%) is retained hindering interpretation of anthropogenic sources with time. However, Kahn and Brush (1994), Cornwell et al. (1996) and Church et al. (2006) found no major change in phosphorus with core depth and profiles tracked changes in loadings over time. Controlling factors that would allow the sediment to retain more phosphorus and limit recycling include rate of sediment accumulation and magnitude of phosphorus loadings.

Nitrogen is transported in rivers and estuaries mostly in the dissolved form and its cycling is much more complex (Meybeck, 1982, Van Breemen et al. 2002; Castro et al., 2003; **Figure 1**). As such, retention of nitrogen in coastal and riverine sediments is potentially more limited than

for phosphorus. As with phosphorus, controlling factors may include the rate of sediment accumulation and the magnitude of nitrogen loading. In addition, the stable isotopes of nitrogen ( $^{14}/^{15}\text{N}$ ) can help determine the source, fate and cycling of nitrogen in a water body and could be reflected in the nitrogen buried in sediments (see Kendall, 1998). For example, Church et al. (2006) showed an increase in  $\delta^{15}\text{N}$  of sediment N with time that is reflective of increases in urbanization in the Delaware Estuary; similar to a variety of studies in other areas (McClelland et al., 1997; Kendall, 1998; Lake et al., 2001; Ulseth and Hershey, 2005).

Sediment cores are extremely useful in determining if various pollution control actions were/are effective in reducing contaminant loadings, as well as providing a time frame for system response (Smol, 2008). In addition, biological material retained in the sediments can help determine changes in ecosystem processes and health (Smol, 2008; Potapova and Charles, 2007; Bennion et al., 2001; Cooper, 1999; 1995; Cooper and Brush, 1993). These proxies such as diatoms and foraminifera can be used to determine changes in response to watershed and estuarine changes in nutrient loadings and concentrations. Hence, coring data are important to determine environmental conditions, identifying some of the effects to the river, how conditions may be improving, and, importantly, and at what rate. This information is especially important for modeling programs in which forecasts are developed by extending past trajectories.

#### *A2: Objectives of Study*

*It is the objective of this study to collect sediment cores from the tidal region of the Murderkill River and determine the chronology of carbon, nitrogen and phosphorus deposition, loadings and related ecological responses.* To meet this objective, we obtained and analyzed the chemical characteristics of sediment cores from depositional areas within the targeted waters. This study aimed to quantify and provide insight into the temporal nature of nitrogen and phosphorus impacts relative to changes within the watershed and loadings of these chemicals. It also sought to understand how the trophic status of the system has changed over decadal time scales.

#### *A3: Study Area*

The Murderkill River Basin occupies 275 km<sup>2</sup> in the southeastern portion of Kent County, DE. The Murderkill River is the main branch of the watershed system and flows approximately



37 km from its headwaters near Felton (DE) to its confluence with the Delaware Bay at Bowers Beach (**Figure 2**). The lower portion from upstream of the Route 113 Bridge at Frederica (DE) to the mouth is tidally influenced and is approximately 5 km in length. The current land use of the watershed is agriculture (55%), wooded/forest (17%), wetlands (6-9%), urban areas (14%) and open water (<2%) (DNREC, 2005).

### *Changes in the Murderkill River Watershed and Nutrient Enrichment*

The water quality of the Murderkill is affected by persistent pollution impacts (i.e., eutrophication and low dissolved oxygen) from agricultural runoff and waste water discharges, in addition to having somewhat restricted hydrography (Aurand and Daiber, 1973; deWitt and Daiber, 1974; DNREC, 2005). Nutrient over-enrichment and low dissolved oxygen are two environmental issues of concern in the Murderkill watershed (DNREC, 2007). Major sources are point source discharges, surface runoff from agricultural fields, animal-raising operations, septic tanks, and historic uses as noted in elevated nitrogen in groundwater discharges. In the mid to late 1970s, a large wastewater treatment plant was constructed in Frederica (DE) which, at the time, had a planned mean daily discharge of  $38 \times 10^3 \text{ m}^3$  (de Michele, 1972 as cited in deWitt and Daiber, 1974). Currently, there is one major discharger (Kent County Facility, DE0020338) and two minor (Harrington STP and Canterbury Crossing MHP) to the river. The Kent County facility discharges ( $\sim 11$  MGD;  $\sim 42 \times 10^3 \text{ m}^3/\text{day}$ ) directly to the tidal portion of the Murderkill River. Ullman et al (2010) estimate 2007 loads from the Kent County facility based on discharge monitoring reports. Total external (new) loads of N and P to the tidal portion vary over the year. Nitrogen loads in 2007 ranged from 20 to 110 metric tons per month and were mainly derived from upstream watershed inputs with lesser amounts from atmospheric deposition and the Kent County Waste Water Treatment Plant (WWTP). Phosphorus loads to the tidal waters ranged from 0.5 to 8 metric tons per month in 2007 with  $>\sim 80\%$  derived from the Kent County WWTP and lesser amounts from the watershed and atmospheric deposition.

Historically, the tidal waters of the sub-estuary are considered to have abnormally low rates of dissolved oxygen (deWitt and Daiber, 1974) of between 63 to  $\sim 90 \mu\text{M O}_2$  during the summertime. In addition, Aurand and Daiber (1973) measured substantial concentrations of dissolved nitrate of between 40 to  $100 \mu\text{M N}$  in winter decreasing to 5 to  $20 \mu\text{M}$  in the summer. This is most likely the results of agricultural and animal raising operations. Current

concentrations of dissolved inorganic N (DIN) ranged from 100 to 300  $\mu\text{M}$  N in the tidal river (fall, 2008) and, for dissolved inorganic P (DIP), from 2 to 8  $\mu\text{M}$  P. The river is currently listed on Delaware's 303(d) list of impaired waters (DNREC, 2005; 2007) due to high bacteria levels, low dissolved oxygen and excessive nutrients. Based on modeling analyses, both point and non-point sources of nitrogen and phosphorus and organic material (i.e., BOD) need to be reduced to meet Delaware water quality standards and targets. In 2005, EPA and DNREC implemented a TMDL for excess nutrient inputs to the river (high and low flow conditions). Monitoring shows that 310-450 kg of N and 130-153 kg of P are discharged daily into the river (US EPA, 2005) from the Kent County facility. The waste load allocation for the facility, set by a TMDL, was 340 kg N/day and 28 kg P/day (reduction of 80%) with compliance gauged on a monthly basis (DNREC, 2006).

In general, there is a lack of historical water monitoring data, i.e., from the 1940s/1960s to the present, to assess the changes in land use and nutrient addition on the water quality (e.g., dissolved oxygen, plant ecology, marsh dynamics) of the tidal river. The goal of this project is to obtain a historical perspective on nutrient inputs and ecological response into the Murderkill River using dated sediment cores, and to evaluate whether pollution controls have been effective.

## **B) Field and Laboratory Methods**

### *B1: Field Sampling*

Sediment cores were collected on October 10, 2008 by staff from The Academy of Natural Sciences and University of Delaware (UDEL) at four locations in the tidal river (**Figure 2; Table 1**). Overall, eight cores were obtained and all provided good sediment chronologies (based on  $^{210}\text{Pb}$  and  $^{137}\text{Cs}$ , see below).

Cores were collected on the marsh surface during mid to low tide. Core locations were from the interior of the marsh, away from any obvious disturbances (e.g., creek banks and ditching). At each site two cores were obtained, one for chemical analysis and the other for stratigraphic descriptions of each site. Push-piston cores of approximately 1 to 1.5 m in length were retrieved by a tripod/pulley system (**Figure 3**). The cores were taken to the laboratory and sectioned into specific intervals (e.g., 2 cm). Samples were stored in pre-cleaned jars at  $-10^{\circ}\text{C}$  at either Academy or UDEL facilities. Chain-of custody procedures were followed from the time of collection, shipping and until the analyses were completed.

## B2: Laboratory Methods

Laboratory clean-techniques were used throughout and are well published (Church et al., 2006; US EPA, 1995; APHA, AWWA and WEF, 1995) using well accepted protocols as outlined in standard operating procedures (SOPS) at the Academy of Natural Sciences and University of Delaware. All materials coming in contact with the samples were either glass or metal that were cleaned of any contaminants prior to use. Sample ID forms were used and each sample was given a unique laboratory number for sample tracking.

Sediments were analyzed for the following parameters at laboratories operated by the Academy of Natural Sciences (Patrick Center): organic carbon, total nitrogen and total phosphorus, and stable isotopes of carbon and nitrogen. In addition, specific sections were analyzed for diatoms via sample digestion, mounting and glass slide light microscopy. Sediments for radioisotope analysis ( $^{210}\text{Pb}$  and  $^{137}\text{Cs}$ ) were analyzed at University of Delaware (Center for Earth, Oceans and Environment). Below are brief descriptions of each chemical, biological, or physical method.

### **B2.1: Radioisotope Measurements and Sedimentation Rates**

In the laboratory, sediment cores were extruded vertically and sectioned in 2-cm intervals for analysis. Sediment bulk density ( $\rho_d$ ) and loss-on-ignition (LOI) measurements were made for each core section to aid interpretation of the downcore radionuclide and chemical data. Dry-bulk density was calculated from porosity ( $\phi$ ) using representative values of interstitial fluid density ( $\rho_f$ ) and mineral density ( $\rho_m$ ) according to:

$$\rho_d = (1 - \phi) \rho_m \quad (1)$$

where  $\rho_m = 2.65 \text{ g/cm}^3$ . Porosity was computed gravimetrically from water content ( $W_c$ ) and using an assumed pore water density of  $\rho_f = 1.0 \text{ g/cm}^3$ :

$$\phi = \left( \frac{W_c \rho_m}{W_c \rho_m + (1 - W_c) \rho_f} \right) \quad (2)$$

where  $W_c = W_{\text{wet}} - W_{\text{dry}} / W_{\text{wet}}$ . Dry sediment weight was determined by drying the sectioned wet sediment in a convection oven at  $100^\circ\text{C}$  for 24 h. The dry sediment was then ground to a fine powder for LOI determination and radionuclide analysis.

LOI measurements were used to quantify the relative proportion of organogenic (combustible) and minerogenic (residual ash) materials in the sediments. Following the method of Heiri et al. (2001), a 4-g quantity of sample power was combusted at 550°C in a muffle furnace for 4 h. LOI was computed as follows:

$$LOI = \frac{W_{dry} - W_{ash}}{W_{dry}} \cdot 100\% \quad (3)$$

where  $W_{dry}$  is the weight of sample previously dried at 100°C, and  $W_{ash}$  is the weight of the residual ash.

To develop sediment chronologies and determine accretion rates for the sediment column, measurements of  $^{210}\text{Pb}$  ( $t_{1/2}=22.3$  years) and  $^{137}\text{Cs}$  ( $t_{1/2}=30.1$  years) were made by gamma spectroscopy of the 46.5 and 661.6 keV photopeaks, respectively (Cutshall et al., 1983; Wallbrink et al., 2002). Powder samples were placed in a 60-ml plastic jar and counted for 24-48 h on a Canberra Model 2020 low-energy Germanium detector (LEGe). The radionuclide concentration (activity) of excess  $^{210}\text{Pb}$  was determined by subtracting the activity of its parent nuclide  $^{214}\text{Bi}$  (609.3 keV) from the total activity. Detector efficiencies were determined from counts of NIST Standard Reference Material 4357 (Inn et al., 2001). The counting geometry of the core samples was kept identical to that of the NIST standard such that a self-absorption correction for  $^{210}\text{Pb}$  was not necessary. Confidence limits reported with radioisotope data are the propagated one-sigma background, calibration, and counting errors.

Three approaches were used to reconstruct the accumulation history of marsh deposits. Two of these methods are based on downcore profiles of  $^{210}\text{Pb}$  activity, and the third uses the depth distribution of  $^{137}\text{Cs}$  activity. The first approach, the constant activity model (CA), assumes that the specific activity of  $^{210}\text{Pb}$  (dpm/g) deposited remains constant through time. In other words, variations in mineral sedimentation rate do not affect the initial concentration of  $^{210}\text{Pb}$ . At steady state, excess  $^{210}\text{Pb}$  decreases exponentially with depth in the sediment column following:

$$A = A_o \exp(-\lambda z/S) \quad (4)$$

where  $A$  is the excess activity of  $^{210}\text{Pb}$  at depth  $z$ ,  $A_o$  is the initial activity of excess  $^{210}\text{Pb}$ ,  $\lambda$  is the decay constant for  $^{210}\text{Pb}$  (0.3114 years), and  $S$  is the vertical accretion rate. The slope of the regression line of  $\ln A$  versus  $z$  is proportional to the accretion rate with dimensions length/time. In this method the age of a sediment interval is derived from a single value of  $S$  averaged over

the  $^{210}\text{Pb}$  profile. The corresponding mass accumulation rate, with the dimensions mass/area/time, is determined by plotting  $A$  as a function of cumulative mass, the depth-integrated product of  $\rho_d$  and  $z$ .

The second method, the constant flux model (CF), relates time and accretion rate to the inventory of excess  $^{210}\text{Pb}$  by assuming that the flux of  $^{210}\text{Pb}$  to the sediments (rather than  $A_o$  concentration) is constant. Sediment age and  $^{210}\text{Pb}$  are related as:

$$I = I_o \exp(-\lambda t) \quad (5)$$

where  $I$  is the inventory of excess  $^{210}\text{Pb}$  below depth  $z$  (dpm/cm<sup>2</sup>),  $I_o$  is the total inventory of excess  $^{210}\text{Pb}$  in the sediment column, and  $t$  is the sediment age at depth  $z$ . Radionuclide inventories of excess  $^{210}\text{Pb}$  (and  $^{137}\text{Cs}$ ) are computed as:

$$I_o = \sum_i \rho_{di} x_i A_i \quad (6)$$

where  $\rho_d$  is the dry-bulk density,  $x$  is the sediment thickness,  $A$  is the radionuclide activity, and the  $i$  operator indicates the  $i$ th depth interval. In the CF model, sediment accretion rates are computed by dividing the length of the dated sediment column by the corresponding age in years.

The third chronological method is based on the first occurrence of  $^{137}\text{Cs}$  in the sediment column as an absolute indicator of ca. 1954, the year of  $^{137}\text{Cs}$  introduction to the global atmosphere by nuclear weapons testing (Ritchie and McHenry, 1990). The depth of  $^{137}\text{Cs}$  penetration divided by the interval between ca. 1954 and the year of core collection is used to compute an average accretion rate. The corresponding mass accumulation rate is determined by plotting  $^{137}\text{Cs}$  activity against cumulative mass. The advantage of  $^{137}\text{Cs}$  chronology over  $^{210}\text{Pb}$  dating methods is that it more closely approximates the absolute age of sediments deposited after ca. 1954.

Both the CA and CF  $^{210}\text{Pb}$  models have been widely used to develop sediment chronologies for tidal marsh deposits, but they are based on different assumptions that are not met in all types of depositional environments. The CF model assumes that 1) all  $^{210}\text{Pb}$  deposited is derived from direct atmospheric deposition, and 2) variations in  $A_o$  are due to changes in the minerogenic sediment accumulation rate  $S$  as opposed to changes in  $^{210}\text{Pb}$  supply (Appleby and Oldfield, 1978). In other words, a change in  $S$  through time will be met by a corresponding change in  $A_o$  in accordance with Equation 5. This model was originally developed for lake systems and thus is most appropriate for depositional environments that sequester  $^{210}\text{Pb}$  mostly (if not exclusively)

through direct atmospheric deposition. Although tidal marshes are exposed to the atmosphere most of the time, tidal flooding brings particle-bound  $^{210}\text{Pb}$  from coastal waters that can increase  $A_o$  above that supplied by the atmospheric flux. For this study we computed sediment accretion and accumulation rates using both  $^{210}\text{Pb}$  models but place more weight on the CA approach, because the assumptions are less restrictive regarding  $^{210}\text{Pb}$  sources.

The following conditions are implicit in all  $^{210}\text{Pb}$  and  $^{137}\text{Cs}$  dating methods: 1) mixing by burrowing organism has not enhanced particle burial; 2) the modeled radionuclide is chemically immobile; and 3) the sedimentary record is complete and not punctuated by non-depositional or erosional episodes. As elaborated later, these assumptions appear to have been met in this study for all cores.

### **B2.2: Total Organic Carbon and Total Nitrogen**

Total organic carbon and total nitrogen were measured using a CE Flash Elemental Analyzer following the guidelines in EPA 440.0, manufacturer instructions and ANSP-PC SOP. Samples were pre-treated with acid to remove inorganic carbon.

### **B2.3: Total Phosphorus**

Total sediment phosphorus was determined using a dry oxidation method modified from Aspila et al. (1976) and Ruttenberg (1992). Solubilized inorganic phosphorus was measured with standard phosphate procedures using an Alpkem Rapid Flow Analyzer. Standard reference material (spinach leaves) and procedural blanks were analyzed periodically during this study. All concentrations were reported on a dry weight basis.

### **B2.4: Stable Isotopes of Carbon and Nitrogen**

The stable isotopic composition of sediments was analyzed using a Finnigan Delta XL coupled to an NA2500 Elemental Analyzer (EA-IRMS). Samples were run in duplicate or triplicate with the results reported in the standard  $\delta$  (‰) notation:  $\delta X = (R_{\text{sample}}/R_{\text{standard}} - 1) \times 1000$ ; where X is either  $^{13}\text{C}$  or  $^{15}\text{N}$  and R is either  $^{13}\text{C}/^{12}\text{C}$  or  $^{15}\text{N}/^{14}\text{N}$ . The  $\delta^{15}\text{N}$  standard was air ( $\delta^{15}\text{N} = 0$ ), and for  $\delta^{13}\text{C}$  the standard is the Vienna PeeDee Belemite (VPDB) limestone that has been assigned a value of 0.0 ‰. Analytical accuracy was based on the standardization of the UHP  $\text{N}_2$  and  $\text{CO}_2$  used for continuous flow-IRMS with IAEA N-1 and N-2 for nitrogen and

IAEA sucrose for carbon, respectively. An in-house calibrated sediment standard was analyzed every tenth sample. Generally, precision based on replicate sample analysis was better than 0.2‰ for carbon and 0.6‰ for nitrogen.

## **B2.5: Diatoms**

About 1-g core sediment was subsampled and the organic component was oxidized with 70% nitric acid while heated in a CEM microwave (165°C) for 1.5 h. Diatoms were repeatedly allowed to settle for 24 hours and the supernatant was decanted until it reached a neutral pH. A measured amount of digested sample was dripped onto a microscope cover slip and dried. Cover slips were then mounted onto slides using a high refractive index mounting medium (Naphrax™). Diatoms were counted and identified using a Leica DM LB2 microscope equipped with DIC optics. At least four hundred valves were counted for each slide at 1000x magnification, unless diatom concentration was too low to allow a 400-valve count. More details on standard Phycology Section operating procedures for diatom analysis can be found in “Protocols for the analysis of algal samples collected as part of the USGS National Water Quality Assessment Program” (Charles et al., 2002; <http://diatom.ansp.org/nawqa/protocols.asp>). Diatom species identifications were made using the extensive diatom library at ANSP (Charles et al., 2002). Several diatom community metrics were calculated based on species autecological preferences originally assembled by van Dam et al. (1994). Metrics were calculated using the Phyco-Aide program developed at ANSP. Assemblages in each core were analyzed using Principal Component Analysis (PCA). The scores of each taxon along PCA axis 1 were used to order the sequence of taxa in diatom stratigraphic profiles.

## **C) Results and Discussion**

### *C1: Sediment Bulk Properties and Sediment Accumulation*

The activity of  $^{210}\text{Pb}$  and  $^{137}\text{Cs}$  (reported as disintegrations per minute per gram of sediment; dpm/g) with depth can be used to determine the sedimentation rate and historical record of contaminants in sediments (Simpson et al., 1983; Orson et al., 1990; 1992; Valette-Silver, 1993; Appleby, 2001; Smol, 2008; Ridgway and Shimmield, 2002; Sommerfield, 2006). This information can be used for the construction of sediment budgets (Schubel and Hirschberg, 1977;

Brush et al., 1982; Officer et al., 1984) and to understand chemical/nutrient accumulation in aquatic environments (Owens and Cornwell, 1995; Cornwell et al., 1996; Latimer and Quinn, 1996; Van Metre and Callender, 1997; Church et al., 2006; Velinsky et al., 2007; 2010; Hatzwell et al., 2010). Also, dated sediment cores can provide information as to the changes in loadings of contaminants over time (e.g., Rippey and Anderson, 1996; Santschi et al., 2001). Such information is especially useful in tracking the effectiveness of various management actions designed to reduce inputs to specific areas (Owens and Cornwell, 1995; Zhang et al., 1993). However, there are many variables that can affect the usefulness of  $^{210}\text{Pb}$  and  $^{137}\text{Cs}$  dating in a given area (Appleby and Oldfield, 1978; Crusius and Anderson, 1991; Appleby, 2001). These include mixing of the sediment by benthic organisms (i.e., burrowing organisms), physical mixing from dredging and storm events, post-depositional movement of contaminants and of the  $^{210}\text{Pb}$  or  $^{137}\text{Cs}$ , and additional inputs of  $^{210}\text{Pb}$  from sources in the landscape (i.e., sediment focusing). The cores obtained in this study provided excellent chronologies of sediment deposition and accumulation. For historical analysis, the sediment accumulation rates derived from the Constant Activity (CA) model for  $^{210}\text{Pb}$  were used to produce an age-depth relationship. The results provides linear rates from approximately 1920s to the present. For dates prior to the 1920s we assume linear rates to the bottom of the cores. While this is useful for this analysis, we are less confident in the dating at the bottom of the cores due to effects associated with compaction, non-linear sedimentation rates, and other factors (Neubauer et al., 2002; Sommerfield, 2006).

### **C1.1: Sediment Properties**

All of the cored deposits consisted of clayey silt with variable quantities of living and dead plant material. Dry-bulk densities ranged from 0.11 to 0.76 g/cm<sup>3</sup> overall. Each location exhibited slightly a different distribution with increasing depth (**Figures 4-7; Tables 2-5**). It is expected that with depth there would be an increase in dry bulk density as burial compaction of the sediment column results in the expulsion of porewater; however, this trend was not evident in all cores. Core MK-1 exhibited a bimodal distribution in the upper 40 cm with a slight decrease with depth, similar to core MK-2. Core MK-3 decreased slightly from the surface to approximately 20 cm, then was variable to 80 cm and sharply increased towards the bottom.



Bulk densities in core MK-4 decreased from the surface to approximately 20 cm, then increased to a maximum at 50-52 cm, after which it decreased slightly towards the bottom.

The amount of organic material in the cores ranged from 9.6 to 71%; values representative for marsh deposits in general (**Figures 4-7; Tables 2-5**). While the loss on ignition (LOI) varied substantially with depth in the cores across the sites, in general, %LOI was higher in the upper river cores (MK-1 and MK-2) compared to the lower sites. In the upper river sites, LOI was as high as ~70%. In MK-1, concentrations remained fairly constant (~27%) near the surface then increased sharply between 60 and 40 cm and remained higher (~52%) to the core bottom. A similar increase occurred in MK-2 (between 60 and 40 cm) as %LOI increased towards the bottom, up to 71%. In core MK-3, %LOI was highest at surface (~50%), decreasing towards the bottom (<15%), similar to MK-4. However, concentrations remained fairly constant below approximately 25 cm in core MK-4.

In general, LOI varied inversely with dry-bulk density and suggests that depth variations in sediment bulk density are partly due to the concentration of organogenic material. In summary, the physical properties data suggest that in the upper two stations there was a major change in sediment type and material deposited over time. Other chemical and biological indicators reflect changes as well (see below).

### **C1.2: Accretion and Sediment Accumulation Rates**

Excess  $^{210}\text{Pb}$  profiles for MK-1 exhibited a monotonic decrease in the log of the activity downcore, indicative of steady-state sediment accumulation and radioactive decay (**Figure 4**). The accretion rate determined using the Constant Activity (CA) model was 0.74 cm/yr and the corresponding mass accumulation rate was 0.20 g/cm<sup>2</sup>/yr. The  $^{137}\text{Cs}$  activities increased upcore from the depth of first occurrence at 44-48 cm to a sharp peak at 28-32 cm, above which activities decreased to lower, but detectable, values near the core top (**Figure 4; Table 2**). The shape of the profile is consistent with the source function for the mid-Atlantic region (Olsen et al., 1981). At this site accretion and mass accumulation rates calculated from the depth of peak  $^{137}\text{Cs}$  activity are 0.71 cm/yr and 0.19 g/cm<sup>2</sup>/yr, respectively.

Core MK-2 exhibited  $^{137}\text{Cs}$  and  $^{210}\text{Pb}$  distributions that were similar to those observed for core MK-1 (**Figure 5; Table 3**). The  $^{137}\text{Cs}$  activities increased upcore from the depth of first occurrence at 44-48 cm to a distinct maximum centered at 28-32 cm, and then decreased to near-

zero activities at the core top. There was  $^{137}\text{Cs}$  activity measured below the stated 44-48 cm onset depth, at 52-56 cm, but  $^{137}\text{Cs}$  values return to zero after this deeper point and it is therefore considered inaccurate as a result of chemical diagenesis. Accretion and mass accumulation rates based on the  $^{137}\text{Cs}$ -peak are 0.71 cm/yr and 0.12 g/cm<sup>2</sup>/yr, respectively. Excess  $^{210}\text{Pb}$  accretion rates at this site are 0.74 cm/yr and 0.13 g/cm<sup>2</sup>/yr.

Core MK-3 had an abrupt first occurrence of  $^{137}\text{Cs}$  at 32-36 cm, maximum activity at approximately 16-20 cm, and decreasing activities to the core top (**Figure 6; Table 4**). Accretion and mass accumulation rates derived using  $^{137}\text{Cs}$ -peak data were 0.44 cm/y and 0.10 g/cm<sup>2</sup>/yr, respectively. Excess  $^{210}\text{Pb}$  profile is similar to cores MK-1 and MK-2, producing an accretion rate of 0.60 cm/yr and a mass accumulation rate of 0.14 g/cm<sup>2</sup>/yr.

The first occurrence of  $^{137}\text{Cs}$  activity in core MK-4 was at 20-22 cm, with a broad peak present at 8-16 cm (**Figure 7; Table 5**). This site has accretion and mass accumulation rates of 0.31 cm/yr and 0.16 g/cm<sup>2</sup>/yr from  $^{137}\text{Cs}$ -peak activity, respectively. Excess  $^{210}\text{Pb}$  follows the distribution of the other cores, but the monotonic decrease in the log of the activity becomes more variable near the bottom of the sampled depth (30-50 cm). Accretion and mass accumulation rates calculated from the excess  $^{210}\text{Pb}$  activity are 0.33 cm/yr and 0.17 g/cm<sup>2</sup>/yr, respectively. Core MK-4 was located at a slightly higher elevation than the other sites, which may have an effect on the lower accumulation rates seen here.

The rates calculated from the excess  $^{210}\text{Pb}$  method are used in the depth-age models later in this report, and the  $^{137}\text{Cs}$  rates corroborate these findings very well. The  $^{210}\text{Pb}$  and  $^{137}\text{Cs}$  accretion rates vary by less than 10% for every core except MK-3. This suggests sediment accumulation has been more-or-less invariant over the period of interest. An important observation is the presence of measurable  $^{137}\text{Cs}$  activity at the tops of all cores. Given that the global atmospheric flux of  $^{137}\text{Cs}$  has been negligible since the early 1980s, this pattern implies that previously deposited  $^{137}\text{Cs}$  has been redistributed in the system. Wash-in of soil-bound  $^{137}\text{Cs}$  from the watershed and (or) erosion of subtidal deposits can account for redeposition of  $^{137}\text{Cs}$  in river-estuaries. Additionally, bioturbation can rework  $^{137}\text{Cs}$  from depth, but the shapes of the  $^{210}\text{Pb}$  and  $^{137}\text{Cs}$  profiles determined for this study are not suggestive of intense biological mixing.

**Table 6** provides the summary information and models for the radioisotopes for the Murderkill cores. Accretion rates, based on  $^{210}\text{Pb}$ , ranged from 0.74 cm/yr at MK-1 and MK-2 to almost 0.33 cm/yr at MK-4. These rates are well within the range of accretion throughout the

tidal Delaware Estuary (Sommerfield and Velinsky, 2010). At 14 sites in the estuary spanning tidal fresh to marine, the range of accretion rates is 0.3 to 1.3 cm/yr with an average of  $0.50 \pm 0.4$  cm/yr (n=32 cores).

In summary, cores MK-1 through MK-4 yielded reliable accretion rates with good agreement between  $^{137}\text{Cs}$  and  $^{210}\text{Pb}$  chronological methods. Because the monotonic decrease in the log of the  $^{210}\text{Pb}$  activity fits each core with such precision,  $^{210}\text{Pb}$ -derived accretion rates derived from **Tables 2-6** were used to convert sediment depths to ages for the nutrient-eutrophication histories. Dates corresponding to depth intervals within the individual cores appear in **Tables 2-6**. These estimates are a key output of this project and allow us to place the nutrient data into a historical context.

### **C1.3: Radionuclide Inventories and Focusing Factors**

Sediment inventories of excess  $^{210}\text{Pb}$  and  $^{137}\text{Cs}$  were computed to compare the relative amount of radionuclide deposited among the four coring sites (MK-1 through MK-4). Reference inventories of 28 dpm/cm<sup>2</sup> for  $^{210}\text{Pb}$  and 21 dpm/cm<sup>2</sup> for  $^{137}\text{Cs}$  are known from direct measurements of radionuclide atmospheric deposition in the U.S. mid-Atlantic region (Olsen et al. 1985; Graustien and Turekian, 1986). These reference values represent the total amount of radionuclide that could be buried at a site if supplied by atmospheric deposition alone.

The focusing factor is the ratio of the measured and reference radionuclide inventory. Focusing is the process by which fine-grained materials migrate towards more depositional areas and provide higher inventories than predicted by reference inventories. To account for this migration, a focusing factor was calculated by comparing the actual  $^{210}\text{Pb}$  inventory to the expected  $^{210}\text{Pb}$  inventory. A focusing factor greater than unity implies that radionuclide activity has been preferentially transported or "focused" from one location to another by a combination of hydrodynamic flow and sedimentary processes. Conversely, a focusing factor less than unity implies that the atmospheric flux is not sequestered locally perhaps on account of sediment erosion and redistribution. In the case of  $^{210}\text{Pb}$ , tidal flooding of a brackish or saline marsh can supply  $^{210}\text{Pb}$  in addition to that derived by atmospheric deposition because coastal and estuarine waters usually contain  $^{210}\text{Pb}$  activity from atmospheric as well as non-atmospheric sources. This is not the case in a tidal freshwater system, where all of the  $^{210}\text{Pb}$  is atmospherically supplied, and focusing occurs through lateral transport of particle-bound  $^{210}\text{Pb}$ .  $^{137}\text{Cs}$  can be focused in a

similar manner as  $^{210}\text{Pb}$ , although  $^{137}\text{Cs}$  is less particle reactive than  $^{210}\text{Pb}$  and tends to desorb from sedimentary particles in brackish and saline waters. Consequently, sediment inventories of  $^{137}\text{Cs}$  in freshwater systems tend to be higher than those in estuaries and coastal waters. This must be taken into account when interpreting  $^{137}\text{Cs}$  focusing factors for sites that span a wide range of salinities.

Radionuclide inventories and focusing factors for the four coring sites (MK-1 through MK-4) are presented in **Table 6**. Site MK-2 had the second lowest excess  $^{210}\text{Pb}$  inventory and the highest  $^{137}\text{Cs}$  inventory among the sites sampled. The  $^{210}\text{Pb}$  focusing factor of 1.69 indicates that the sediment column has been accretionary for the period of interest, and that atmospheric deposition is not the only source of radionuclide. This site had a  $^{137}\text{Cs}$  focusing factor of 0.48, indicating a deprivation of  $^{137}\text{Cs}$ . The trend in  $^{210}\text{Pb}$  and  $^{137}\text{Cs}$  inventories at MK-2 was to be expected, given the generally freshwater setting of the site. However, site MK-1 is farther upstream than MK-2 and had the highest  $^{210}\text{Pb}$  inventory and the second lowest  $^{137}\text{Cs}$  inventory among the sites. The  $^{210}\text{Pb}$  focusing factor of 2.35 suggests that non-atmospherically derived radionuclide is deposited at this site, perhaps supplied by tidal waters and/or from eroding sediment in the upstream freshwater source. Since MK-1 and MK-2 are separated by less than 1 km, it is possible that the source of  $^{210}\text{Pb}$  enrichment to MK-1 also affects MK-2. Site MK-3 had the lowest  $^{210}\text{Pb}$  inventory and a  $^{137}\text{Cs}$  inventory that was second only to site MK-2. The  $^{210}\text{Pb}$  focusing factor of 1.6 suggests influx of radionuclide from tidal estuarine waters. Another possibility is that soil-bound  $^{210}\text{Pb}$  eroded from the surrounding landscape and focused at the site. Site MK-4 had radioisotope inventories and focusing factors within the range of values measured at the other sites.

The similar  $^{137}\text{Cs}$  focusing factors at the four depositional sites suggest that the Murderkill system is a mixed marsh where  $^{137}\text{Cs}$  is scavenged everywhere, not just in saline water near the entrance to Delaware Bay. The  $^{210}\text{Pb}$  focusing factors make clear that the four depositional sites have sequestered  $^{210}\text{Pb}$  inventory at levels 1.6 to 2.35 times greater than what can be accounted for by atmospheric flux alone. This result confirms that most of the minerogenic material buried at these sites is allochthonous (i.e., transported to the location from elsewhere), and implies that atmospherically sourced, particle-reactive constituents in the Murderkill River system will exhibit focusing patterns that depend not only on broad scale atmospheric delivery but also on more regional and local transport processes (e.g., tidal flow and sediment transport). An

important point is that all of the coring sites, while depositional, are subject to both small and large scale processes (i.e., within the tidal waters and from the watershed) that influence radioisotope and nutrient profiles.

## *C2: Nutrients/Eutrophication*

### **C2.1: Sediment Total Carbon, Total Sediment Nitrogen and Total Sediment Phosphorus**

Sediment organic carbon (SOC) concentrations for the four cores ranged between 2.3% and 34.3% on a dry weight basis (dw) with an average of  $13.4 \pm 8.1\%$  SOC ( $\pm 1\sigma$ ); **Tables 7-10; Figure 8**). Similarly, total nitrogen (TN) ranged from 0.21 to 1.7% N with an overall average of  $0.68 \pm 0.37\%$ ; while total sediment phosphorus (TSP) ranged from 0.03 to 0.21% TSP with an overall average of  $0.07 \pm 0.03\%$ . Similar concentrations were found for TN and TSP in marsh cores taken from the river in the summer of 2007 (Chesapeake Biogeochemical Associates, 2007)

Sediment total nitrogen concentrations were highest in the bottom half of the cores from MK-1 and MK-2 (**Figure 8**). At MK-1, TN decreased from 50 to 40 cm and then remained fairly constant towards the surface. A similar change occurred in MK-2 except that concentrations increased from 25 cm to the surface. In both MK-3 and MK-4, TN concentrations remained fairly constant in the entire core. A similar distribution was observed for SOC in all cores (**Figure 8**). SOC concentrations were highest in the bottom sections of the MK-1 and MK-2 (up to 34%) decreasing to lower concentrations by 40 cm with MK-2 also showing an increase to the surface. Concentrations of TOC in MK-3 were intermediate to those upstream and downstream (range of 3.4 to 24%). Total sediment P (TSP) increased slightly towards the surface in all cores, with the greatest increase observed in MK-4 (**Figure 8**). Concentrations of TSP were generally  $< 0.1\%$  below 10 cm, increasing towards the surface.

The carbon to nitrogen ratio (C/N; atomic units) can be used as a tracer of the source of organic matter to a location and potential diagenetic changes that could occur during burial (Jasper and Gagosian, 1990; Meyers, 1994; Prahl et al., 1994). Diagenesis is any chemical, physical, or biological change undergone by sediment after its initial deposition (Bernier, 1980; Burdige, 2006). For example, terrestrial material (e.g., trees) are rich in cellulose (i.e., higher C) compared to algae or marsh plants that have less structural material and are higher in proteins (i.e., higher N). Typical marine plants have C to N ratios of  $\sim 4$ -10 while terrestrial material can

have C to N values > 15-20. Diagenesis of recent sediments tends to increase the C to N ratio due to preferential remineralization and release of nitrogen compounds; however, re-incorporation of bacterially derived N can increase the C to N ratio over time (Fogel et al., 1989; Benner et al.; 1991). In the upstream MK-1 core (**Figure 8**), the C/N ratio was only slightly higher at depth (18 versus ~24) suggesting preferential loss of nitrogen with burial, while at MK-2 there was no substantial change downcore (C/N of  $24 \pm 2$ ). The carbon to nitrogen ratio at MK-3 revealed slightly higher values in the surface (up to 40 at 24-26cm), decreasing with depth. Lastly, at MK-4, the C to N ratios was fairly constant with depth ( $18.5 \pm 2.8$ ) except for the upper section in which the C/N was 30.4.

### **C2.2: Stable Isotopes of Carbon and Nitrogen**

Organic carbon and nitrogen isotopic ratios are useful to distinguish between marine and continental plant sources of sedimentary organic matter, processing and cycling of nutrients and, in some instances, the level of system-wide productivity (Fry, 2006 and others). Most photosynthetic plants incorporate carbon into organic matter using the C3 Calvin pathway, which biochemically discriminates against  $^{13}\text{C}$  to produce a  $\delta^{13}\text{C}$  shift of about -20‰ to -30‰ from the isotope ratio of the inorganic carbon source. C4 plants (e.g., corn, *Spartina*) incorporate  $\text{CO}_2$  using a different system (PEP) that discriminates against  $^{13}\text{C}$  to produce a  $\delta^{13}\text{C}$  shift of about -8‰ to -15‰ from the isotope ratio of the inorganic carbon source. Organic matter produced from atmospheric  $\text{CO}_2$  ( $\delta^{13}\text{C} \sim -7\text{‰}$ ) by land plants and typical of a tidal freshwater wetlands, using the C3 pathway consequently has an average  $\delta^{13}\text{C}$  (PDB) value of about -27‰ (O'Leary, 1988). The source of inorganic carbon for marine algae (C3 plants) is dissolved bicarbonate, which has a  $\delta^{13}\text{C}$  value of about 0‰. Marine organic matter consequently typically has  $\delta^{13}\text{C}$  values between -20‰ and -22‰. The isotopic difference between organic carbon produced by C3 land plants and marine algae has been used to trace the delivery and distribution of organic matter to sediments in estuarine and coastal areas (Cifuentes et al., 1989; Fogel et al. 1992, and many others).

Carbon isotope ratios can be affected by photosynthetic dynamics and by postdepositional diagenesis (Dean et al., 1986; Fogel et al., 1992; Canuel et al., 1995; Zimmerman and Canuel, 2002) and consequently must be interpreted cautiously. A big factor that can impact  $\delta^{13}\text{C}$  values of plant material is the availability of  $\text{CO}_2$  and rate of production during photosynthesis and the

possibility of selective diagenesis of organic matter fractions that are isotopically heavy or light. While the change in  $\delta^{13}\text{C}$  appears to be small ( $<2\text{‰}$ ) during recent diagenesis (Hayes et al., 1989; Meyers, 1994), shifts due to the availability and rate of production, due to nutrient enrichment or limitation and other factors, can have a large impact on the resultant  $\delta^{13}\text{C}$  values of deposited organic matter (Fogel et al., 1992; Schelske and Hodell, 1995; Church et al., 2006).

Differences exist between the natural abundances of stable nitrogen isotopes ( $\delta^{15}\text{N}$ ,  $^{15}\text{N}/^{14}\text{N}$ ) in dissolved and particulate matter from terrestrial, estuarine, marine, and anthropogenic sources (Kendall, 1998 and others). Terrestrial-occurring soil nitrogen can have a wide range of values, but in general range from  $-1$  to  $+4\text{‰}$  similar to atmospheric nitrogen ( $0\text{‰}$ ). Nitrogen isotopic compositions from marine sources tend to be slightly enriched in the heavier isotope ( $^{15}\text{N}$ ) and are very dependent on the source of dissolved nitrogen and its  $\delta^{15}\text{N}$ , and processing in the system (e.g., ammonification, nitrification, denitrification, etc) at the time of formation. A dominant process in many aquatic environments (and groundwater) is denitrification (Cline and Kaplan, 1975). Denitrification is a microbially facilitated process of dissimilatory nitrate reduction that ultimately produces molecular nitrogen ( $\text{N}_2$ ) through a series of intermediate gaseous nitrogen oxide products. This microbial process uses dissolved nitrate during oxidation of organic matter and as nitrate is consumed there is an enrichment of residual nitrate in the system. Algal/plant production and its  $\delta^{15}\text{N}$  from nitrate would reflect the balance between processes and inputs. There are many points in which nitrogen can be fractionated and its isotopic composition altered. For example, wastewater from treatment facilities has been shown to increase the  $\delta^{15}\text{N}$  of various fish species (Lake et al., 2001) due to the selective removal of the light isotope ( $^{14}\text{N}$ ) nitrogen during treatment. Anthropogenic nitrogen was substantially enriched in watersheds with greater amount of urbanization and wastewater inputs and the nitrogen was shown to be incorporated into the aquatic food web (McCelland et al., 1997).

The isotopic compositions of sediment C and N exhibited interesting changes within each core, especially the two upper river sites (**Figure 9**). The carbon isotopic composition of the sediment ranged from  $-27$  to  $-19\text{‰}$  ( $\delta^{13}\text{C}$  average of  $-17.6\text{‰}$ ). In cores MK-1 and MK-2, the  $\delta^{13}\text{C}$  was lowest in the bottom sections of the core below  $40\text{ cm}$  ( $\sim -27\text{‰}$ ) (**Figure 9**). In each of these two cores, the sediment organic matter become enriched in  $^{13}\text{C}$  reaching a  $\delta^{13}\text{C}$  of  $-17$  and  $-15\text{‰}$  at the surface. These changes were not present in cores from MK-3 and MK-4. At both

sites the  $\delta^{13}\text{C}$  was fairly constant (except in the very bottom of core MK-3), averaging  $-16\pm 0.6\text{‰}$  and  $-15\pm 0.6\text{‰}$ , respectively.

The  $\delta^{15}\text{N}$  of the sediment increased towards the surface to varying degrees in all cores (**Figure 9**). As with the carbon isotopic signatures, at sites MK-1 and MK-4 the  $\delta^{15}\text{N}$  started to change at around 40 cm, increasing towards the surface. In core MK-1, the  $\delta^{15}\text{N}$  was  $\sim 1\text{‰}$  near the bottom increasing to  $10\text{‰}$  at the surface. Similarly, at MK-2, the  $\delta^{15}\text{N}$  increased to approximately  $8\text{‰}$  near the surface. In cores MK-3 and MK-4 the increase in  $\delta^{15}\text{N}$  towards the surface was less pronounced. For example, at MK-4 the  $\delta^{15}\text{N}$  increased from approximately  $1.8\text{‰}$  in the bottom 40cm to approximately 3 to  $4.5\text{‰}$  at the surface.

### **C2.3: Diatom Analysis and Assemblages**

Diatoms are microscopic, photosynthetic algae with a siliceous structure. They contain yellow-brown pigments and therefore are also referred to as golden algae. Comprising one of the most common types of algae, they are found in a diverse range of environments from freshwater to marine. Diatoms species are differentiated by their shape and characteristics of their siliceous structure. The main forms are centric (i.e., circular, radial symmetry), and pennate (i.e., having bilateral symmetry). They exhibit two main living modes in the environment: planktonic and benthic (i.e., living on or in the bed sediment).

Diatoms are one of the most powerful water quality indicators; they colonize virtually every aquatic microhabitat and many diatom species have very strict ecological requirements, with well-defined optima and tolerances for environmental variables such as pH, nutrient concentration, salinity, water transparency and physical habitat. Because of their strong relationships with environmental conditions, diatoms are used to derive inference models for such environmental factors. The inference models are developed using calibration sets of both diatoms and measured environmental variables for specific geographic regions. In order to produce robust quantitative models, the calibration sets require a large number of sampling sites that maximize the gradient length covered by the variable of interest (e.g., phosphorus concentration, pH, etc.). These models can then be used to infer the environmental parameter of interest when instrumental measurements are not available, and have been successfully used to reconstruct reference conditions and assess the impact of anthropogenic activities on aquatic systems (e.g., Cooper et al., 1993; 1995; Bennion et al., 2001).



Diatom assemblages have been shown to be important indicators of nutrient concentration within freshwater and marine environments. Due to the fact the diatoms respond quickly and directly to nutrients, they have been used for many years as indicators of nutrient changes in aquatic systems (Potapova et al., 2004; Potapova and Charles, 2007; Ponader et al., 2008). In this study we take a first approach using metrics calculations based on models developed by van Dam et al. (1994). While this data set is mostly based on freshwater species it does contain some marine diatoms. It provides ecological information for both diatoms and water characteristics is not currently available for the Delaware Estuary.

A total of 56 sections were analyzed for diatom composition from four Murderkill River cores (MK-1, MK-2, MK-3, and MK-4). At least 400 valves were counted for each sample and over 300 taxa (**Appendix I**) were identified in these samples allowing a robust analysis for nutrient and ecological conditions. The distribution of key diatom species (those occurring with more than 5% relative abundance) in each of the cores is presented in **Figures 10-13**. Brief descriptions of the species' stratigraphic distribution and major shifts in diatom assemblages are provided below for each core.

**Core MK-1:** 215 species were identified in 15 sections from core MK-1, of which only 19 species occurred with abundances > 5% in at least one sample. The most abundant species were: *Stauroforma exiguiformis* (maximum relative abundance 66%), *Cymatosira belgica* (32%), *Navicula salinarum* (17%), *Denticula subtilis* (16%), *Nitzschia brevissima* and *N. frustulum* (10%). In this core two distinct types of diatom assemblages were present: one with the species *Stauroforma exiguiformis* dominant and rarer benthics such as *Nitzschia nana*, *Pinnularia subcapitata* occurring between the core bottom and 42-44 cm core depth. This freshwater, circumneutral to slightly acidic type of diatom assemblage was replaced above 42-44 cm by an assemblage with a much more diverse species composition, mostly represented by brackish-marine taxa such as *Cymatosira belgica*, *Navicula salinarum*, *Denticula subtilis*, *Nitzschia brevissima*, *Cyclotella striata* (**Figure 10**). The major shift to brackish-marine diatom species took place in the mid to late 1950s.

**Core MK-2:** 172 species were identified in 14 sections from this core with 21 species > 5% relative abundance in at least one sample. The most abundant species were: *Stauroforma*

*exiguiformis* (maximum relative abundance 71%), *Pseudostaurosira subsalina* (28%), *Navicula salinarum* (22%), and *Diploneis smithii* (22%) (**Figure 11**). Similar to core MK-1, a major shift from freshwater-type diatoms with abundant *S. exiguiiformis* to marine-brackish species took place at 36 cm core depth. The freshwater-type of assemblage differed slightly from core MK-1 by the presence of abundant *D. smithii* amongst other benthic species such as *Pinnularia viridis* and *Calloneis bacillum*) at the core bottom, and species that are usually present in more acidic waters such as *Frustulia saxonica*, and *Eunotia* spp. The major change in diatom assemblages from freshwater to marine took place in the late 1940 to mid 1950s.

**Core MK-3:** In this core, 152 species were identified, of which 21 species were present with relative abundances > 5%. The most abundant species were: *Luticola mutica* (maximum relative abundance 43%), *Caloneis bacillum*, *Paralia sulcata* (14%), *Denticula subtilis* (13%), *Navicula cincta* (12%), *Actynocyclus normanii* fo. *subsalsum*, and *Navicula* sp. 1 MUR DME (10%) (**Figure 12**). Below 28 cm depth of the core, diatom species were very diverse with nutrient-rich freshwater species (*Calloneis bacillum*, *Nitzschia frustulum*) as well as brackish-marine species (*Denticula subtilis*, *Paralia sulcata*). Above 28 cm, a major shift took place with *Luticola mutica*, a subaerial diatom species usually found on rocks and walls, becoming abundant and even dominant in many core sections of this interval. In the upper two sections (0-2 and 4-6-cm intervals), *L. mutica* decreased while marine species such as *A. normanii*, *Cyclotella striata*, and *Cymatosira belgica* increased in relative abundance.

**Core MK-4:** A total of 136 species were identified in 11 sections from this core. Diatom assemblages were very diverse, composed of both marine-brackish and freshwater eutrophic species. No species were dominant in this core except for *Cymatosira belgica* in the top core interval (39%). No particular trend was identified in this core's diatom assemblages either, except that the coastal marine *Cymatosira belgica* displayed increased abundances in both the bottom and upper intervals (**Figure 13**).

The samples collected in the Murderkill River wetlands span a range of marine-brackish to freshwater diatom species, making detailed analysis complex. To extract the ecological information contained in the diatom data identified in this region, various metrics were

calculated for salinity, pH, nitrogen uptake metabolism, and the trophic state (van Dam et al., 1994; USGS NAWQA; Hall and Smol, 1999). These metrics are often used to assess freshwater systems rivers and streams in the U.S. All of these metrics have strengths and weaknesses that vary with the quality of the ecological information available for the taxa found in each of the cores. Because most marine or brackish species present in the Murderkill River region do not occur in van Dam et al. (1994) data sets, metric calculations were based mostly upon the freshwater species occurring in these cores. The van Dam et al. (1994) summary and synthesis of ecological characteristics of taxa is based primarily on samples from Western Europe, and generally includes taxa with wide geographic distributions. The van Dam et al. (1994) autecological values for many taxa have been revised to be more relevant for the U.S., and are contained in a data compilation developed for the USGS National Water Quality Assessment (NAWQA) program by Porter (2008) and Porter et al. (2008). To allow a comparison between the current study in the tidal Murderkill River and the previous studies of the tidal Christina River and Saint Jones River (Velinsky et al., 2007; 2010), the data set and metrics by van Dam et al. (1994) will be the focus of this discussion.

The van Dam et al. (1994) diatom metrics show an abrupt increase in the proportion of eutrophic species (i.e., high nutrient species) in cores MK-1, MK-2, and MK-3, starting at 42-44 cm, 34-36 cm, and 18-20 cm towards the surface of the core, respectively (**Figure 14; Tables 11-14**). Below this depth range, oligotrophic, freshwater species are present in MK-1 and MK-2, while in MK-3, diatom species are mostly mixed meso- and eutrophic species, with a small spike in oligotrophic species at 70 cm depth. Core MK-4 mainly displays an increasing (but fluctuating) trend in eutrophic species, except for the top two intervals.

To evaluate how nutrient conditions, as reflected by total sediment N and P, impacted the diatom species and metrics in each core, N and P were plotted against the metrics for eutrophic species (**Figures 15-16**). For cores MK-1 and MK-2, there was an inverse relationship ( $r^2 = 0.74$  and  $r^2 = 0.73$  for MK-1, and MK-2, respectively) between eutrophic species (as per Van Dam et al., 1994) and TN (i.e., the higher the TN, the lower the %eutrophic diatoms; **Figure 15**). In core MK-3 there was a slight positive trend while there was no relationship observed in MK-4. In all cores, there was no relationship between TSP and the diatom trophic metric (**Figure 15**). The accumulation rate of N and P (see below) were calculated and plotted against the %eutrophic diatoms as this might be a better integrator of N and P inputs to the river. As

with the concentration data there was no consistent relationship between the N or P accumulation rate (over time) and changes in the trophic status of the tidal river.

The trends observed in diatom autecology and sediment stable isotopes reveal the complexity of nutrient inputs and biogeochemical processes taking place within the tidal Murderkill River, and suggest that more elaborate analyses of data are necessary to reveal their dynamics. For example, cross-correlation analyses are necessary to account for the lag response between changes in nutrients and shifts in diatom species, or to account for lags related to sedimentary nutrient re-mobilization. However, within the Murderkill river system, the upper part of cores MK-1 and MK-2 reveal a shift in diatom species related to increasing nutrient concentration which clearly correlates with the positive trend observed in  $\delta^{15}\text{N}$  curves that may be related to post-war increasing anthropogenic effects. A similar change, but much more recent was observed in core MK-3, while core MK-4 did not reveal a particular trend in nutrient concentration.

### *C3: Historical Analysis*

A major focus of this study was to determine the changes in the loadings of nitrogen and phosphorus over time within the tidal Murderkill River system. These changes are thought to have occurred in the early to mid 1970s with the introduction of wastewater from the Kent County Waste Water Treatment facility (KC WWTP) that came online during this time period. In addition, an objective was to determine if there was any indicator of an ecosystem change (e.g., change in plant flora, oxygen dynamics, marsh production, etc.) as a result of the facility and effluent discharges of nitrogen and phosphorus. Lastly, we wanted to determine if the marshes along the tidal river are a sink for N and P via sediment burial and how this relates to other inputs.

It is important to recognize that both nitrogen and phosphorus can undergo substantial biogeochemical processing and diagenetic changes during burial (**Figure 1**). In brief, inorganic forms of N and P are taken up by marsh plants, phytoplankton and benthic algae and incorporated into marsh sediments. During burial, microbial activity (both oxic and anoxic) can release organic nitrogen and phosphorus into the porewaters of the sediments which can move back into the overlying waters. A major sink or loss reaction for nitrogen is denitrification which converts oxidized nitrogen to nitrogen gas which is then removed from the system. These nutrients, along with externally introduced nutrients, are then transported downstream or taken

up again during photosynthesis. This recycling of nutrients in a marsh is a major process that impacts overall marsh/estuarine productivity and transport to coastal areas. In this regard, depending on the environment and specific characteristics, such as the magnitude of nutrient loadings, sedimentation rates, oxic/anoxic conditions, it may or may not be possible to measure changes in nitrogen or phosphorus accumulation rates that reflect inputs from external sources such as with chemicals that do not undergo significant biogeochemical reactions (e.g., PCBs, Pb, Zn, etc).

### **C3.1. Changes in Nutrients and Diatoms in Murderkill River Cores.**

In the tidal Murderkill, total nitrogen in sediments over time varied between core locations (**Figure 17**). At the upper station (MK-1), TN concentrations were highest between 1900 and 1920 (~ 1.5% N), decreasing to approximately 0.6% N by 1940 and remaining constant to the present. A similar change occurred at MK-2 but the concentrations started to increase after approximately 1970, near the same time as the KC WWTP came online. This location was in the main river just downstream from the small tributary/canal in which the treatment plant discharges. At both MK-3 and further downstream at MK-4, TN concentrations were fairly constant from 1900 to the present. However, concentrations in the near surface sections were highest at MK-2 and decreased downstream.

The stable isotopes of sediment nitrogen may give some indication as to changes in the source of nitrogen and biogeochemical cycling within the tidal river. Ulseth and Hershey (2005), Leavitt et al. (2006) and Velinsky (unpublished data) show that higher  $\delta^{15}\text{N}$  of the nitrogen is associated with higher inputs from urban sources and waste water. Bratton et al. (2003) showed similar trends in cores from the Chesapeake Bay. Lastly, in Woodbury Creek (NJ) and Oldmans Creek marshes an increase in  $\delta^{15}\text{N}$  of the nitrogen was observed in marsh sediment cores and attributed to both increase nitrogen loading and changes in the way nitrogen is processed in wastewater treatment plants (Church et al., 2006). Downcore variations of  $\delta^{15}\text{N}$  are somewhat difficult to interpret given the number of biogeochemical processes influencing nitrogen. In the Murderkill marshes, there was a pronounced increase in the  $\delta^{15}\text{N}$  of the sediment nitrogen in MK-1, MK-2 and MK-3 and to a lesser degree in MK-4 (**Figure 17**). The increase in the  $\delta^{15}\text{N}$  of the sediment nitrogen, from approximately  $< 1.0\text{‰}$  to 3 to 10‰ presently, started in the 1940s substantially before the increase in wastewater loadings to the estuary. The low  $\delta^{15}\text{N}$  prior to the

1940s in the upstream areas suggest more terrestrial sources (Kendall, 1998) of N which would be around 0 to +2‰, while the higher values downstream at MK-4 are influenced by marine sources which tend to be higher. In this regard, Elliot and Brush (2006) showed a correlation between the  $\delta^{15}\text{N}$  of tidal wetland core sediments and estimate of nitrogen wastewater loadings over time. However, it is unclear what may have occurred in the Murderkill watershed during this time period to substantially increase the  $\delta^{15}\text{N}$ , but it is most likely a combination of changes that occurred during this time period (e.g., population and septic system increases to changes in the biogeochemical cycling of nitrogen).

Concentrations of total sediment phosphorus (TSP) changed over time at all locations to some degree (**Figure 18**), especially at MK-4. At MK-1, concentrations were slightly higher from approximately 1900 to 1940 ( $0.075 \pm 0.01\% \text{P}$ ,  $n=4$ ), decreased to  $0.71 \pm 0.01\% \text{P}$  ( $n=12$ ) from 1940 to 2003, with a slight increase at the surface ( $0.11\% \text{P}$ ). At MK-2 concentrations were similar until approximately 1980 at which time concentrations increased  $0.12\% \text{P}$ . A similar trend, but at lower concentrations, was observed at MK-3 with concentrations reaching only  $0.09\% \text{P}$  at the surface. The largest change was observed further downstream at MK-4 (**Figure 18**). At this location, TSP was constant from the 1900s to 1970 after which concentrations substantially increased to  $0.15$  to  $0.20\% \text{P}$  in 2008. While the increase in concentrations at MK-2 and MK-3 may be a result of the discharge starting in the 1970s, it is unclear why the largest increase was observed much farther downstream at MK-4. It is possible that drainage of water from the large wetlands area upstream of Old Brockonbridge Gut (near South Bowers Beach; **Figure 1**) imparts a large load of phosphorus to the main river and that a portion of this phosphorus is deposited on the marsh platform adjacent to the tidal gut.

Schelske and Hodell (1991; 1995), and Perga and Gerdeaux (2004) have shown a relationship between the concentration of P in the sediments or water and the isotopic composition of carbon ( $\delta^{13}\text{C-OC}$ ) in the sediments or in fish scales over time. The fish scales were an integrator of the top of the pelagic food web (i.e., phytoplankton). Recently, Church et al. (2006) showed a similar trend and relationship in a sediment core from Woodbury Creek, NJ. In brief, it is proposed that as P levels increase, primary productivity increases to a point at which there is reduced isotopic fractionation during enzymatic uptake of dissolved  $\text{CO}_2$ . This reduced fractionation would result in higher isotopic compositions of organic matter (i.e., more  $^{13}\text{C}$ -enriched) and would suggest that P was helping to control aquatic productivity. Therefore, if

phosphorus is limiting production, the  $\delta^{13}\text{C}$  of the organic carbon in a core may reflect a system-wide change in productivity. In the Murderkill River, at only the upper two locations (MK-1 and MK-2) was there a significant enrichment of  $^{13}\text{C}$  in the sediments of the core over time.

Sediment  $\delta^{13}\text{C}$  changed from approximately -25‰ to ~ -15‰ from the 1900s to the present. In both downstream cores there was only a slight change throughout the entire core with an overall average of  $-15.4 \pm 1.1\text{‰}$ . There was no relationship between TSP and  $\delta^{13}\text{C}$  of the organic carbon, suggesting that phosphorus may not be limiting in this system and that other factors are controlling the  $\delta^{13}\text{C}$  of the organic carbon in the sediments (see below). It is possible that changes in the source of organic matter to the marshes (i.e., terrestrial-upland material versus *in situ*-local production), or that *in situ* marsh processes and plant communities may have changed over time.

The diatom metrics used to assess eutrophication for each core are plotted against time in **Figure 19**. It appears that there are two separate trends occurring in the cores from the various sites over time. At MK-1 and MK-2 there is a distinct increase in the index for eutrophic conditions starting in the late 1930s, early 1940s. The index then decreased in the late 1950s and increased slightly after the 1970s. At MK-3, there was no increase in the late 1930s but there was a gradual increase in the late 1960s—early 1970s which maybe an indicator of the increase in nitrogen and phosphorus loadings from various sources including the KC WWTP. There was no substantial change in the eutrophic index at MK-4 over time.

One major change that occurred in cores from MK-1 and MK-2 was a shift from freshwater species of diatoms to more marine/estuarine species starting in the 1950s (**Figure 10 and 11**). That is, a major shift from freshwater-type diatoms (e.g., *S. exiguiformis*) to marine-brackish species. Other freshwater-benthic diatoms included abundant *D. smithii*, and *Pinnularia viridis* and *Calloneis bacillum*) at the core bottom. Species common in more acidic waters such as *Frustulia saxonica* and *Eunotia* spp were also present. These were replaced by brackish-marine taxa such as *Cymatosira belgica*, *Navicula salinarum*, *Denticula subtilis*, *Nitzschia brevissima*, and *Cyclotella striata*. This shift was not evident farther downstream at MK-3 and MK-4.

### C3.2 Changes in Marsh Ecology

In addition to the change in diatom flora, there was a large shift in the stable isotopic composition of carbon and nitrogen during this time period (i.e., 1930s to the present; **Figures 17**

**and 18).** The changes in the  $\delta^{13}\text{C}$  of the organic carbon over time indicate that the marsh shifted from C3 dominant plants (e.g., wild rice, spatterdock, and others) to C4 dominant plants (e.g., *Spartina* sp.). *Spartina* species have  $\delta^{13}\text{C}$  values enriched in  $^{13}\text{C}$ , characteristic of plants using the C4 photosynthetic pathway (Smith and Epstein, 1971). Separate analysis of *Spartina alterniflora* from the Murderkill River yielded a  $\delta^{13}\text{C}$  of  $-13.7 \pm 0.4\text{‰}$  (n=4), close to the values exhibited in the surface sediment of all cores. While there are some C3 saltmarsh plants (e.g., *Scirpus* sp.) that have been shown to have more negative  $\delta^{13}\text{C}$  values (Cloern et al., 2002; Chmura and Aharon, 1995), it is unclear how dominant this plant was in the past. Plants typically present in a tidal freshwater marsh (e.g., wild rice, *Typha*, spatterdock, and others) use the C3 photosynthetic pathway and have  $\delta^{13}\text{C}$  values enriched in  $^{12}\text{C}$  (i.e., more negative  $\delta^{13}\text{C}$ ) (Cloern et al., 2002; Chmura and Aharon, 1995). The presence of freshwater diatoms and the more negative  $\delta^{13}\text{C}$  of the sedimentary organic matter in the bottom section of these two cores suggest that before 1940, these two marshes were predominately tidal freshwater. Byrne et al. (2001) showed that changes in water storage and diversion in the San Francisco Estuary resulted in changes in diatoms and carbon isotopic composition of a sediment core from a tidal marsh. A similar change could be occurring in the Murderkill River.

The exact cause of this shift is unclear, but it is hypothesized that the hydrology changed in the tidal river such that more saline water moved upstream over time. Presently, salinities range from 1-5 psu to 10-15 psu over the year at the Route 1 Bridge, just upstream from MK-1 (USGS monitoring data, unpublished). It is possible that the salinities in the upper region were fresher in the past (see for example Byrne et al., 2001). The increase in salinity around the two upstream sites initiated a shift from a marsh dominated by C3 plants (i.e., more typical of a tidal freshwater wetland) to a salt marsh with a dominance of *Spartina*, that took place from the 1940s to 1960s. There are two possibilities that may have caused this change: damming of upstream flows and reduced freshwater inputs, and the increase tidal prism as a result of mosquito ditching during the early to mid-1930s. While there is little information concerning the timing and extent of tributary damming upstream, there are three dams: McGinnis Pond on Hudson Branch, Killen and Coursey Pond on Upper Murderkill River, and Andrews Lake on Pratt Branch. It is thought that these ponds are old mill ponds created to produce local energy and were created prior to the 1900, however more information is needed to confirm the timeframe. Bourn and Cottam (1950) as cited by Clarke et al. (1984) stated that during the 1930s, approximately 90% of the Atlantic



coastal marshes were grid-ditched to drain surface water where the pesky mosquito breeds. Ditches were dug at 50- to 100-m intervals throughout various marshes. Within the Murderkill River, aerial photographs from 1937 show the presence of ditches throughout the lower reaches of the river ([www.datamil.delaware.gov](http://www.datamil.delaware.gov)). Since the digging of the mosquito ditches and changes in marsh organic matter and diatom flora occurred during the same time period, it is suggested that ditching allowed salt water to move farther upstream in the tidal river. LeMay (2007) showed that mosquito ditches can change the way the marsh drains and floods but did not investigate the hydrologic impact to the larger river system. It is possible that the ditches increased the tidal prism of the river and allowed saline water to move further upstream. In either case, the marshes upstream at MK-1 and MK-2 experienced a change from a freshwater biota to a more marine biota and this change needs to be further investigated.

### **C3.3: Nitrogen and Phosphorus Accumulation Rates**

Sediment cores can be used to calculate the mass of nitrogen (N) and phosphorus (P) accumulating in the marsh over time. Using the mass accumulation rate (MAR) and concentration of nitrogen and phosphorus (% TN and %TSP) in each interval, the N and P accumulation rate (mg N or P/cm<sup>2</sup>-yr) for each year can be obtained. It should be noted that missing intervals that were not analyzed for N and P were linearly interpolated from the interval concentrations above and below. The accumulation rates can then be applied to estimate of wetland area to provide an estimate of the amount of N and P removed (via burial) by wetland processes. Other removal/transport processes (e.g., denitrification, recycling, sediment movement) would need to be determined to provide a complete N and P cycle in the river.

Nitrogen accumulation rates for the four locations presently range from approximately 1 to 2.5 mg N/cm<sup>2</sup>-yr (**Figure 20**). At MK-1, MK-2 and MK-3, rates were ~ 2 mg N/cm<sup>2</sup>-yr before the 1960s decreasing to a minimum in 1970 then increasing from approximately 1970/1975 to the present. At MK-4 there was no minimum but a small increase over time to the present. Phosphorus accumulation rates exhibited a similar pattern with time in the cores (**Figure 20**), except there was no minimum present (except possibly MK-2). In general, starting after approximately 1975, P accumulation increased from 0.05 to 0.1 mg P/cm<sup>2</sup>-yr to 0.15 to 0.3 mg P/cm<sup>2</sup>-yr at the present. Again the timing in core MK-2 was slightly later than in the other three cores. However, these changes do reflect and correspond to the timing when the KC WWTP

starting discharging to the tidal river. These rates and the change over time are similar to those found in a tidal freshwater wetland in Patuxent River (Kahn and Brush, 1994) and in marshes along the Patuxent salinity gradient (Hartzell et al., 2010).

A rough estimation of the area of tidal wetlands is 4,300 acres ( $1.74 \times 10^7 \text{ m}^2$ ; DNREC, 2005). Using this area and the surface values for N and P accumulation yields current burial rates (gross rates) of  $25 \times 10^6 \text{ g N/month}$  and  $3.4 \times 10^6 \text{ g P/month}$ , respectively. Ullman et al. (2010) estimated monthly N and P external loading to the tidal Murderkill Estuary from the KC WWTP, upstream loads from the watershed and direct atmospheric loads. Nitrogen loadings (predominately from the upper watershed) ranged from approximately 20 to  $100 \times 10^6 \text{ gN/month}$  while P loads (predominately from the KC WWTP) ranged from  $< 0.5$  to  $13 \times 10^6 \text{ gP/month}$ . These calculations show that marsh accumulation can sequester a majority of the P and N loads from the various sources. However sediment recycling of N and P (Berner, 1980; Buridge, 20086) are not accounted for in these estimates and will modify and most likely reduce these fluxes. In this regard, Ullman et al. (2010) estimated that the tidal river may not be attenuating phosphorus substantially while nitrogen may be significantly removed from processes such as denitrification and burial within the estuary and not exported to the Delaware Bay. However, the estimates provided above show that the marshes have a potential to trap both N and P before export to the tidal river.

## D) Summary and Conclusions

This study involved the chemical analysis of four sediment cores taken from the tidal Murderskill River in Kent County, DE. These cores were taken from upstream near Frederica to downstream (near Bowers Beach) and were dated using  $^{210}\text{Pb}$  and  $^{137}\text{Cs}$  radiometric methods. All cores provided sufficient temporal coverage ( $> 50$  yr) for detailed chemical analysis. The main objective was to evaluate historical trends in nutrients (i.e., sediment phosphorus and nitrogen) and evaluate if a historical record of eutrophication could be derived from algal analysis (i.e., diatom species in the cores) along with other indicators of potential ecosystem change (e.g., stable isotopes of carbon ( $\delta^{13}\text{C-OM}$ ) and nitrogen, ( $\delta^{15}\text{N-TN}$ )).

The range and average sediment accumulation rates ( $^{137}\text{Cs}$ ) inferred from the  $^{210}\text{Pb}$  and  $^{137}\text{Cs}$  data are similar to other areas within the Delaware Estuary and range from 0.33 to 0.74 cm/yr (based on  $^{210}\text{Pb}$ , constant accumulation model). There was good agreement between the  $^{137}\text{Cs}$  rates and those for the constant accumulation model for  $^{210}\text{Pb}$ .

Sediment organic carbon (SOC) concentrations for the four cores ranged between 2.3% and 34.3% on a dry weight basis (dw) with an average of  $13.4 \pm 8.1\%$  SOC ( $\pm 1\sigma$ ). Similarly, total nitrogen (TN) ranged from 0.21 to 1.7% N with an overall average of  $0.68 \pm 0.37\%$ ; while total sediment phosphorus (TSP) ranged from 0.03 to 0.21% TSP with an overall average of  $0.07 \pm 0.03\%$ . Similar concentrations were found for TN and TSP in marsh cores taken from the tidal river in the summer of 2007 (Chesapeake Biogeochemical Associates, 2007). Sediment nitrogen increased in only MK-2 while TSP showed only a small increase towards the surface. Sediment N and P accumulation rates did increase towards the surface starting at approximately the mid to late 1970s. This is approximately the same time frame as the discharge of the KC WWTP.

The analysis of the diatom assemblages and metrics indicate a shift toward more eutrophic species starting in the late 1940-1950s (cores MK-1 and MK-2) or 1970s (core MK-3), but not clear trend was observed in core MK-4. Although no significant relationship was found between the eutrophic diatom metrics and the concentration and accumulation rates of nitrogen and phosphorus in the cores, more elaborate statistical analyses are necessary to identify specific trends. For example, cross correlations should be used to account for the lag in diatom response to nutrient changes, or for processes related to sediment nutrient re-mobilization. Also, more

analyses can be conducted on select groups of diatom species known to have stronger relationships with nutrient concentration. The study of sediment cores from Murderkill tidal river revealed an important aspect related to diatom-based inferences: because the assemblages may include many brackish or marine species, little is known about their nutrient and habitat preferences from the literature; further investigations with simultaneous water quality measurements and quantification of diatom species from coastal environments are necessary to better estimate their ecological requirements.

An interesting finding of this study was the shift of diatom flora from freshwater to brackish-marine species with time in cores MK-1 and MK-2, along with a change in the stable isotopic composition of sediment organic carbon. The organic carbon shifted from more negative values to more positive values indicating a change from C3 plants to C4 plants with time. These data suggest a change of salinity in the upper tidal reaches and that these changes shifted the marsh to its current composition in a time frame of a few decades. Further analysis of sediment proxies need to be accomplished, such as benthic foraminifera composition, bromide (an indicator of salinity) of organic matter and additional cores. It is unclear as to what caused this change but it is thought that some hydrological modification occurred that allowed higher salinity water to move upstream. The data could suggest a potential change due to sea level rise and salinity intrusion and changes in marsh ecology. The potential influence of such factors needs to be explored by analyzing relationships between climate and sea level records and the core sediment proxies.

Lastly, N and P accumulation rates over time have increased two fold since approximately 1975-1980 in a similar time frame as loadings from the KC WWTP. Preliminary estimates of marsh burial suggest that current burial rates can remove a substantial fraction of both N and P; however, recycling rates need to be considered for more accurate estimates. This study provides important data and results that can be incorporated into an ecosystem model for the tidal river to help determine changes in water quality.

### **E) Acknowledgments**

We would like to thank Mihaela Enache, Don Charles, Paul Kiry, Dack G. Stuart and Paula Zelanko for field and laboratory assistance and data interpretation. Dr. Mihalea Enache did diatom counts, calculated diatom metrics and provided assistance with report preparation. We appreciate the help of Roger Thomas in field and Robin Davis provided assistance with final report preparation and review.

## F) References

- American Public Health Association, American Water Works Association and Water Environment Federation (APHA, AWWA and WEF). 1995. *Standard Method for the Examination of Water and Wastewater*, 19th Edition. Washington, DC.
- Appleby, P.G. 2001. Chronostratigraphic techniques in recent sediments: Chapter 9. In: W.M. Last and J.P. Smol (eds). *Tracking Environmental Change Using Lake Sediments Volume 1: Basin Analysis, Coring, and Chronological Techniques*. Kluwer Academic Publishers, Dordrecht, The Netherlands.
- Appleby P.G and F. Oldfield. 1978. The calculation of lead-210 dates assuming a constant rate of supply of unsupported  $^{210}\text{Pb}$  to the sediment. *Catena* 5: 1-8.
- Aspila, K.I, Aspila, H., Agemian A. and Chau, S.Y.,1976. A semi-automated method for the determination of inorganic and total phosphate in sediments. *Analyst* 101: 187-197.
- Aurand, D. and F.C. Daiber. 1973. Nitrate and nitrite in the surface waters of two Delaware salt marshes. *Chesapeake Science* 14: 105-111.
- Bennion, H., P.G. Appleby, and G.L. Phillips. 2001. Reconstructing nutrient histories in the Norfolk Broads: implications for the application of diatom-phosphorus transfer functions to shallow lake management. *Journal of Paleolimnology* 26:181-204.
- Berner, R. 1980. *Early Diagenesis: A Theoretical Approach*. Princeton University Press, 241 pp.
- Benner, R., M. L. Fogel, and E. K. Sprague. 1991. Diagenesis of belowground biomass of *Spartina alterniflora* in salt-marsh sediments. *Limnol. Oceanogr.* 36: 1358-1374.
- Bratton, J.F., S.M. Coleman and R.R. Seal, II. 2003. Eutrophication and carbon sources in Chesapeake Bay over the last 2700 yr.: Human impacts in context. *Geochim. Cosmochim. Acta*. 67: 3385-3402.
- Brush, G.S., E.A. Martin, R.S. DeFries, and C.A. Rice 1982. Comparisons of  $^{210}\text{Pb}$  and pollen methods for determining rates of estuarine sediment accumulation. *Quaternary Research*. 18: 196-217.
- Burdige, D.J. 2006. *Geochemistry of Marine Sediments*. Princeton University Press. 630 pp.
- Bourn, W.S. and C. Cottam. 1950. Some biological effects of ditching tidewater marshes. US Department of Interior, Fish and Wildlife Ser. Res. Rep. 19.
- Boynton, W.R., J.H. Garber, R. Summers, and W.M. Kemp. 1995. Inputs, transformations and transport of nitrogen and phosphorus in Chesapeake Bay and selected tributaries. *Estuaries* 18: 285-314.

- Byrne, R., L. Ingrama, S. Starratta, F. Malamud-Roama, J.N. Collins and M. E. Conrad. 2001. Carbon-isotope, diatom, and pollen evidence for Late Holocene salinity change in a brackish marsh in the San Francisco Estuary. *Quart. Res.* 55: 66-76.
- Canuel, E.A., J.E. Cloern, D.B. Ringelberg, J.B. Guckert and G.H. Rau. 1995. Molecular and isotopic tracers used to examine sources of organic matter and its incorporation into the food webs of San Francisco Bay. *Limnol. Oceanogr.* 40: 67-81
- Castro, M.S., C.T. Driscoll, T.E. Jordan, W.G. Reay and W.R. Boynton. 2003. Sources of nitrogen to estuaries of the United States. *Estuaries and Coasts* 26: 803-814.
- Charles, D. F., Knowles, C., and Davis, R. S. (Eds.). 2002. Protocols for the Analysis of Algal Samples Collected as Part of the U.S. Geological Survey National Water-Quality Assessment Program. Patrick Center for Environmental Research-Phycology Section, The Academy of Natural Sciences of Philadelphia. Report No. 02-06. 124 pp.
- Chesapeake Biogeochemical Associates. 2007. Nutrient Flux Study – July 2007 Results from the Murderkill River-Marsh Ecosystems. Initial Report submitted to Kent County Levy Court (Nov. 2007).
- Church, T.M., C. Sommerfield, D.J. Velinsky, D. Point, C. Benoit, D. Amouroux, D. Plaa and O. Donard. 2006. Marsh sediments as records of sedimentation, eutrophication and metal pollution in the urban Delaware Estuary. *Marine Chemistry* 102(1-2):72-95.
- Chmura, G.L. and P. Aharon. 1995. Stable carbon isotope signatures of sedimentary carbon in coastal wetlands as indicators of salinity regime. *J. Coast. Res.* 11:124-135.
- Cifuentes, L.A., J.H. Sharp and M.L. Fogel. 1988. Stable carbon and nitrogen isotope biogeochemistry of the Delaware estuary. *Limnol. Oceanogr.* 33: 1102-1115.
- Clarke, J.A., B.A. Harrington, T. Hruby, and F.E. Wasserman. 1984. The effect of ditching for mosquito control on salt marsh use by birds in Rowley, Massachusetts. *J. Field Ornithol.* 55: 160-180.
- Cloern, J.E. E.A Canuel and D.Harris. 2002. Stable carbon and nitrogen isotope composition of aquatic and terrestrial plants of the San Francisco Bay estuarine system. *Limnol. Oceanogr.* 47: 713-729.
- Cooper, S.R. 1999. Estuarine paleoenvironmental reconstructions using diatoms. Pages 352 - 373 in Stoermer, E.F. and J.P. Smol, editors. *The diatoms: Applications for the environmental and earth sciences*. Cambridge University Press, Cambridge.
- Cooper, S.R. 1995. Chesapeake Bay watershed historical land use: impact on water quality and diatom communities. *Ecological Applications* 5: 703-723.

Cooper, S. R. and G.S. Brush. 1993. A 2,500-year history of anoxia and eutrophication in Chesapeake Bay *Estuaries* 16: 617-626.

Cornwell, J.C., D.J. Conley, M. Owens, and J.C. Stevenson. 1996. A sediment chronology of eutrophication of Chesapeake Bay. *Estuaries* 19:488-499.

Crusius, J. and R.F. Anderson. 1991. Core compression and surficial sediment loss of lake sediments of high porosity caused by gravity coring. *Limnol. Oceanogr.* 36:1021-1031.

Cutshall, N.H., I.L. Larsen and C.R. Olsen. 1983. Direct analysis of  $^{210}\text{Pb}$  in sediment samples: Self-absorption corrections. *Nuclear Instruments and Methods in Physics Research*, 206: 309-312.

Dean, W.E., Arthur, M.A., and Claypool, G.E., 1986. Depletion of  $^{13}\text{C}$  in Cretaceous marine organic matter: source, diagenetic, or environmental signal? *Mar. Geol.*, 70:119-157.

De Michele, E. 1972. The effects of conservative and non-conservative substances on the Murderkill River. Final Rep., Dept. Nat. Res. Environ. Control; State of De. 101p.

deWitt, P. and F.C. Daiber. 1974. The hydrography of the Murderkill Estuary, Delaware. *Ches. Sci.* 15: 84-85.

DNREC. 2007. State of Delaware 2006 Combined Watershed Assessment Report (305b) and Determination for Clean Water Act Section 303(d) List of Waters needing TMDLs. State of Delaware Department of Natural Resources and Environmental Control Division of Water Resources, Watershed Assessment Section. Dover, DE.

DNREC 2006. Fact Sheet (November 1, 2006). Surface Water Discharge Section; Dover, DE.

DNREC, 2005. Technical Analysis for Amendment of the 2001 Murderkill River TMDLs. State of Delaware Department of Natural Resources and Environmental Control Division of Water Resources, Watershed Assessment Section. Dover, DE (Updated March 1, 2005).

Elliott, E.M. and G.S. Brush. 2006. Sedimented organic nitrogen isotopes in freshwater wetlands record long-term changes in watershed nitrogen source and land use. *Environ. Sci. Technol.* 40: 2910–2916.

Fogel, M.L., L.A. Cifuentes, D.J. Velinsky and J.H. Sharp. 1992. The relationship of carbon availability in estuarine phytoplankton to isotopic composition. *Marine Ecol. Prog. Ser.* 82: 291-300.

Fogel, M.L., E.K. Sprague, A.P. Gize and R.W. Frey. 1989. Diagenesis of organic matter in Georgia salt marshes. *Estuarine, Coastal Shelf Sci.*, 28: 211-230.

Follmi, K.B. 1996. The phosphorus cycle, phosphogenesis and marine phosphate-rich deposits. *Earth Science Reviews* 40: 55-124.



Froelich, P.N., M.L. Bender, N.A. Luedtke, G.R. Heath, and T. De Vries. 1982. The marine phosphorus cycle. *Amer. Jour. Sci.* 282: 474-511.

Fry, B. 2006. *Stable Isotope Ecology*. Springer Science+Business Media, LLC, New York.

Graustein, W.C. and K.K. Turekian. 1986.  $^{210}\text{Pb}$  and  $^{137}\text{Cs}$  in air and soils measure the rate and vertical distribution of aerosol scavenging. *J. Geophys. Res.*, 91: 14,355-14,366.

Hall, R. I., and J. P. Smol. 1999. Diatoms as indicators of lake eutrophication. Pages 128-168 in: E. F. Stoermer, and J. P. Smol (editors). *The diatoms: applications for the environmental and earth sciences*. Cambridge University Press, Cambridge, UK.

Hartzell, J.L., T.E. Jordan, and J.C. Cornwell. 2010. Phosphorus burial in sediments along a salinity gradient of the Patuxent River, a sub-estuary of the Chesapeake Bay. *Estuaries and Coasts* 33: 92-106.

Hayes, J.M, Popp, B.N., Takigiku, R., and Johnson, M.W., 1989. An isotopic study of biogeochemical relationships between carbonates and organic carbon in the Greenhorn Formation. *Geochim. Cosmochim. Acta*, 53:2961-2972.

Heiri, O., A.F. Lotter and G.Lemcke. 2001. Loss on ignition as a method for estimating organic and carbonate content in sediments: reproducibility and comparability of results. *Journal of Paleolimnology*. 25: 101-110.

Hornberger, M.L., S.N. Luoma, A.Green, C. Fuller, and R. Anima. 1999. Historical trends of metals in the sediments of San Francisco Bay, California. *Marine Chemistry*. 64:39-55.

Inn and others 2001. The NIST natural-matrix radionuclide standard reference material program for ocean studies. *Journ. Radioanal. Nucl. Chem.* 248: 227-231.

Jasper, J.P. and R.B. Gagosian. 1990. The sources and deposition of organic matter in the Late Quaternary Pigmy Basin, Gulf of Mexico. *Geochim. Cosmochim. Acta*. 54: 1117-1132.

Jordan, T.E., J. C. Cornwell, W.R. Boynton, and J.T. Anderson. 2008. Changes in phosphorus biogeochemistry along an estuarine salinity gradient: The iron conveyer belt. *Limnol. Oceanogr.* 53: 172-84.

Kahn, H. and G.S. Brush. 1994. Nutrient and metal accumulation in a freshwater tidal marsh. *Estuaries* 17: 345-360.

Kendall, C. 1998. Tracing nitrogen sources and cycling in catchments. In: *Isotope Tracers in Catchment Hydrology*; Elsevier, Amsterdam, pp. 519-576.

- Lake, J.L., R.A. McKinney, F.A. Osterman, R.J. Pruell, J. Kiddon, S.A. Ryba and A.D. Libby. 2001. Stable nitrogen isotopes as indicators of anthropogenic activities in small freshwater systems. *Can. J. Fish. Aquatic Sci.* 58: 870-878.
- Latimer, J.S. and J.G. Quinn. 1996. Historical trends and current inputs of HOCs in an urban estuary: The sedimentary record. *Environ. Sci. Technol.* 30: 623-633.
- Leavitt, P.R., C.S. Brock, C. Ebel and A. Patoine. 2006. Landscape-scale effects of urban nitrogen on a chain of freshwater lakes in central North America. *Limnol. Oceanogr.* 51(5): 2262-2277.
- Lebo, M.E. 1991. Particle-bound phosphorus along an urbanized coastal plain estuary. *Mar. Chem.* 34: 201-216.
- LeMay, L.E. 2007. The impact of drainage ditches on salt marsh flow patterns, sedimentation and morphology: Rowley River, Massachusetts. M.S. Thesis, Virginia Institute of Marine Science, Williamsburg, Virginia, 239 p.
- Litke, D.W. 1999. *Review of Phosphorus Control Measures in the United States and Their Effects on Water Quality*. U.S. Geological Survey, Water Sources Investigations Report 99-4007, National Water Quality Assessment Program, Denver, CO.
- McClelland, J.W., I. Valiela and R.H. Michener. 1997. Nitrogen-stable isotope signatures in estuarine food webs: A record of increasing urbanization in coastal watershed. *Limnol. Oceanogr.* 42: 930-937.
- Meybeck, M. 1982. Carbon, nitrogen and phosphorus transport by world rivers. *Amer. Jour. Sci.* 282: 401-450.
- Meyers, P.A., 1994. Preservation of elemental and isotopic source identification of sedimentary organic matter. *Chem. Geol.* 144: 289-302.
- Mitch, W.J. and J.G. Gosselink. 1993. *Wetlands*, 2<sup>nd</sup> Edition. Van Nostrand Reinhold, NY.
- Neubauer, I.C. Anderson, J.A. Constantine and S.A. Kuehl. 2002. Sediment deposition and accretion in a mid-Atlantic (U.S.A.) tidal freshwater marsh. *Estuarine, Coastal, and Shelf Science*. 54: 713-727.
- Officer, C.B., D.R. Lynch, G.H. Setlock and G.R. Helz. 1984. Recent sedimentation rates in Chesapeake Bay. In: Kennedy, V.S. (ed.). *The Estuary as a Filter*. Academic Press, New York, pp 131-157.
- O'Leary, M.H., 1988. Carbon isotopes in photosynthesis. *Bioscience*, 38:328-336.
- Olsen, C.R., I.L. Larsen, P.D. Lowry, N.H. Cutshall, J.F. Todd and G.T.F. Wong. 1985. Atmospheric fluxes and marsh-soil inventories of <sup>7</sup>Be and <sup>210</sup>Pb. *Journal of Geophysical*

*Research –Atmospheres*. 90: 10487-10495.

Olsen, C.R., H.J. Simpson, T.H. Peng, R.F. Bopp and R.M. Trier. 1981. Sediment mixing and accumulation effects on radionuclide depth profiles in Hudson estuary sediments. *Journal of Geophysical Research*. 86: 11020-11028.

Orson, R.A., R.L. Simpson and R.E. Good. 1992. A mechanism for accumulation and retention of heavy metals in tidal freshwater marshes of the upper Delaware River Estuary. *Estuar. Coast. Shelf Sci.* 34: 171-186.

Orson, R.A., R.L. Simpson and R.E. Good. 1990. Rates of sediment accumulation in a tidal freshwater marsh. *J. Sed. Petrology*. 60: 859-869.

Owens, M. and J.C. Cornwell. 1995. Sedimentary evidence for decreased heavy metal inputs to the Chesapeake Bay. *Ambio* 24: 24-27.

Perga, M.E. and D. Gerdeaux. 2004. Changes in the  $\delta^{13}\text{C}$  of pelagic food webs: The influence of lake area and trophic status on the isotopic signature of whitefish (*Coregonus lavaretus*). *Can. J. Fish. Aquat. Sci.* 61(8): 1485–1492.

Ponader, K.C., D.F. Charles, T.J. Belton and D.M. Winter. 2008. Total phosphorus inference models and indices for coastal plain streams based on benthic diatom assemblages from artificial substrates. *Hydrobiologia* 610: 139-152.

Porter, S.D. 2008. *Algal attributes: An autecological classification of algal taxa collected by the National Water-Quality Assessment Program*: U.S. Geological Survey Data Series 329, 18 p.

Porter, S.D., D.K. Mueller, N.E. Spahr, M.D. Munn and N.M. Dubrovsky. 2008. Efficacy of algal metrics for assessing nutrient and organic enrichment in flowing waters: *Freshwater Biology*. 53: 1036-1054.

Potapova, M. and D.F. Charles. 2007. Diatom metrics for monitoring eutrophication in rivers of the United States. *Ecological Indicators*. 7: 48-70.

Potapova, M., D.F. Charles, K.C. Ponader and D.M. Winter. 2004. Quantifying species indicator values for trophic diatom indices: a comparison of approaches. *Hydrobiologia*. 517: 25-41.

Prahl, F.G., J.R. Ertel, M.A. Goni, M.A. Sparrow and B. Eversmeyer. 1994. Terrestrial organic carbon contributions to sediments on the Washington margin. *Geochim. Cosmochim. Acta*. 58:3035-3048.

Ridgeway, J. and G. Shimmield. 2002. Estuaries as repositories of historical contamination and their impact on shelf seas. *Estuar. Coast. Shelf Sci.* 55: 903-928.

Rippey, B. and H. J. Anderson. 1996. Reconstruction of lake P loadings and dynamics using sedimentary record. *Environ. Sci. Technol.* 30: 1786-1789.

- Ritchie, J.C. and McHenry, R.J. 1990. Application of radioactive fallout Cesium-137 for measuring soil erosion and sediment accumulation rates and patterns: A review. *Journal of Environmental Quality*. 19: 215-233.
- Ruttenberg, K.C. 1992. Development of a sequential extraction method for different forms of phosphorus in marine sediments. *Limnol. Oceanogr.* 37: 1460-1482.
- Santschi, P.H., B.J. Presley, T.L. Wade, B. Garcia-Romero and M. Baskaran. 2001. Historical contamination of PAHs, PCBs, DDTs, and heavy metals in Mississippi River Delta, Galveston Bay and Tampa Bay sediment cores. *Mar. Environ. Res.* 52: 51-79.
- Schelske, C.L. and D.A. Hodell. 1995. Using carbon isotopes of bulk sedimentary organic matter to reconstruct the history of nutrient loading and eutrophication in Lake Erie. *Limnol. Oceanogr.* 40: 918-929.
- Schelske, C.L. and D.A. Hodell. 1991. Recent changes in productivity and climate of Lake Ontario detected by isotopic analysis of sediments. *Limnol. Oceanogr.* 36: 961-975.
- Schubel, J. R. and D. J. Hirschberg. 1977.  $^{210}\text{Pb}$  determined sedimentation rate, and accumulation of metals in sediments at a station in Chesapeake Bay. *Chesapeake Sci.* 18: 379-382.
- Simpson, R.L., R.E. Good, R. Walker and B.R. Frasco. 1983. The role of Delaware River freshwater tidal wetlands in the retention of nutrients and heavy metals. *J. Environ. Qual.* 12: 41-48.
- Smith, B.N. and S. Epstein. 1971. Two categories of  $^{13}\text{C}/^{12}\text{C}$  ratios for higher plants. *Plant Physi.* 47:380-384.
- Smol, J.P. 2008. *Pollution of Lakes and Rivers: A Paleoenvironmental Perspective*- 2<sup>nd</sup> edition. Blackwell Publishing, Oxford.
- Sommerfield, C.K. 2006. On sediment accumulation rates and stratigraphic completeness: Lessons from Holocene ocean margins. *Continental Shelf Research*. 26:2225-2240.
- Sommerfield, C.K. and D.J. Velinsky. 2010. Sediment Accumulation and Marsh Accretion in Tidal Wetlands of a Coastal Plain Estuary. Presented at the 2010 American Geophysical Ocean Sciences Meeting, Portland, OR.
- Sommerfield, C.K. and Madsen, J.A., 2004. Sedimentological and Geophysical Survey of the Upper Delaware Estuary. Final report to the Delaware River Basin Commission, Delaware Sea Grant Publication (DEL-SG-04-04), 124 pp.
- Ulseth, A.J. and A.E. Hershey. 2005. Natural abundances of stable isotopes trace anthropogenic N and C in an urban stream. *JNABS*: 24(2): 270-289.

USEPA 2005. Letter to Mr. Kevin Donnelly from US EPA (August 25, 2005) from Mr. Jon Capacasa, Director, WPD. Decision Rationale: TMDL Analysis for the Murderkill River Watershed, US EPA Region III, Philadelphia, PA

Ullman, W.J., M. Dean, J.R. Scudlark, J. Newton, H. Mirsajadi, A.K. Aufenkampe, R.L. Hays, B. Dzwonkowski, K.C. Wong, T.E. McKenna, and A.S. Andres. 2010. Contrasting loads of nitrogen and phosphorus to and from the Murderkill Watershed and Estuary, Delaware, USA. (11 January 2010) OOB Discussion.

Ulseth, A.J. and A.E. Hershey. 2005. Natural abundances of stable isotopes trace anthropogenic N and C in an urban stream. *JNABS*: 24(2): 270-289.

Valette-Silver, N.J. 1993. The use of sediment cores to reconstruct historical trends in contamination of estuarine and coastal sediments. *Estuaries*. 16: 577-588.

Van Breemen et al. 2002. Where did all the nitrogen go? Fate of nitrogen inputs to large watersheds in the NE USA. *Biogeochemistry* 57/58: 267-293.

van Dam, H., A. Mertens, and J. Sinkeldam. 1994. A coded checklist and ecological indicator values of freshwater diatoms from The Netherlands. *Neth. J. Aquat. Ecol.* 28: 117-133.

Van Metre, P.C. and Callender, E. 1997. Identifying water-quality trends from  $^{210}\text{Pb}$  using dated sediment cores from White Rock Lake Reservoir, Dallas, Texas. *Journal of Paleolimnology*. 17: 239-249.

Velinsky, D.J., Riedel, G.R., J.T.F. Ashley and J. Cornwell. 2010. River sediment investigation near Poplar Point in the tidal Anacostia River, Washington, DC. *Environ. Monitor. Assess* (submitted).

Velinsky, D.J., D.F. Charles and J. Ashley. 2007. Contaminant Sediment Profiles of the St. Jones River Marsh, Delaware: A Historical Analysis. Final Report submitted to DNREC. PCER Report No. 07-05. The Academy of Natural Sciences, Patrick Center for Environmental Research, Philadelphia, PA.

Wallbrink, P.J., D.E. Walling and Q. He. 2002. Radionuclide measurement using HPGe gamma spectrometry. In: F. Zapata (Editor), *Handbook for the Assessment of Soil Erosion and Sedimentation Using Environmental Radionuclides*. Kluwer Academic Publishers, Dordrecht, pp. 67-96.

Zhang et al. 1993

Zimmerman, A.R. and E.A. Canuel. 2002. Sediment geochemical records eutrophication in the mesohaline Chesapeake Bay. *Limnol. Oceanogr.* 47: 1084-1093.

## **Tables**

**Table 1. Core locations and collection dates.**

<b>Name</b>	<b>Abbreviation</b>	<b>Date</b>	<b>Lat (N)</b>	<b>Long (W)</b>	<b>Depth of Core (cm)</b>
Downstream of Bay Rd	MK-1A	10-Oct-08	39° 00.587'	75° 26.963'	73.8
	MK-1B	10-Oct-08	39° 00.584'	75° 26.962'	82.0
Near Outfall Creek	MK-2A	10-Oct-08	39° 00.662'	75° 26.390'	91.0
	MK-2B	10-Oct-08	39° 00.662'	75° 26.391'	94.0
Mid River	MK-3A	10-Oct-08	39° 01.556'	75° 24.751'	98.5
	MK-3B	10-Oct-08	39° 01.555'	75° 24.750'	98.0
Near USGS Gage	MK-4A	10-Oct-08	39° 02.997'	75° 23.523'	104.0
	MK-4B	10-Oct-08	39° 02.998'	75° 23.521'	96.0

Stations are listed from upstream to downstream.

**Table 2. Bulk sediment properties and radioisotope data for MK-1.**

Chem ID	Interval	Water Fraction	Dry Bulk Density (g/cm <sup>3</sup> )	Accumulated Mass (g/cm <sup>2</sup> )	LOI (%)	Total <sup>210</sup> Pb (dpm/g)	Excess <sup>210</sup> Pb (dpm/g)	<sup>137</sup> Cs (dpm/g)	z (cm)	Age Model
	0-2	0.74	0.314	1.29	26.8	8.33	7.71	0.46	2	2005
	2-4	0.73	0.329		26.4				4	2002
	4-6	0.72	0.336	1.30	27.3	7.58	6.85	0.43	6	2000
	6-8	0.74	0.315		28.8				8	1997
	8-10	0.71	0.354	1.51	24.6	8.38	7.54	0.37	10	1994
	10-12	0.68	0.399		21.9				12	1991
	12-14	0.69	0.389	0.78	21.0	7.49	6.55	0.42	14	1989
	14-16	0.68	0.398	0.80	23.1	8.19	6.82	0.52	16	1986
	16-18	0.73	0.328	1.24	23.9	6.91	5.85	0.54	18	1983
	18-20	0.75	0.290		25.7				20	1980
	20-22	0.78	0.253	1.00	27.6	5.23	4.09	1.34	22	1978
	22-24	0.79	0.247		28.6				24	1975
	24-26	0.82	0.197	0.82	33.9	4.30	3.33	1.73	26	1972
	26-28	0.81	0.211		31.1				28	1969
	28-30	0.81	0.217	0.97	29.5	4.16	3.32	2.27	30	1967
	30-32	0.77	0.266		26.4				32	1964
	32-34	0.77	0.271	1.14	26.8	3.05	2.10	0.84	34	1961
	34-36	0.75	0.300		25.8				36	1958
	36-38	0.75	0.297	1.10	26.4	2.15	1.20	0.25	38	1956
	38-40	0.78	0.252		31.3				40	1953
	40-42	0.76	0.280	1.08	28.3	2.30	1.29	0.10	42	1950
	42-44	0.78	0.258		29.6				44	1947
	44-46	0.83	0.187	0.69	39.2	2.68	2.00	0.05	46	1945
	46-48	0.86	0.158		49.7				48	1942
	48-50	0.86	0.152	0.59	56.3	1.30	0.60	-0.04	50	1939
	50-52	0.87	0.145		58.8				52	1936
	52-54	0.86	0.151	0.62	59.7	1.24	1.00	0.06	54	1934
	54-56	0.85	0.161		58.7				56	1931
	56-58	0.86	0.155	0.63	70.5	0.86	0.62	-0.08	58	1928
	58-60	0.86	0.159		60.8				60	1925
	60-62	0.85	0.160		60.6					
	62-64	0.84	0.178		55.9					
	64-66	0.85	0.172		56.5					
	66-68	0.83	0.187		55.1					
	68-70	0.83	0.187		54.6					
	70-72	0.81	0.217		53.8					
	72-74	0.83	0.186		53.0					



74-76	0.82	0.197	51.0
76-78	0.83	0.194	49.8
78-80	0.82	0.198	51.6
80-82	0.83	0.191	49.7

Based on sedimentation Rate (xsPb-210 CA) = 0.74 cm/yr. \*Note: Cells for accumulated mass, total  $^{210}\text{Pb}$ , excess  $^{210}\text{Pb}$  and  $^{137}\text{Cs}$  have been merged in cases where adjacent samples were physically added together for measuring radionuclide activities. For example, MK-1 samples 0-2cm and 2-4cm were dried and combusted separately but combined for radionuclide tests

**Table 3. Bulk sediment properties and radioisotope data for MK-2.**

Chem ID	Interval	Water Fraction	Dry Bulk Density (g/cm <sup>3</sup> )	Accumulated Mass (g/cm <sup>2</sup> )	LOI (%)	Total <sup>210</sup> Pb (dpm/g)	Excess <sup>210</sup> Pb (dpm/g)	<sup>137</sup> Cs (dpm/g)	z (cm)	Age Model
	0-2	0.84	0.180	0.69	51.3	10.91	10.56	0.09	2	2005
	2-4	0.85	0.166		59.3				4	2002
	4-6	0.86	0.159	0.65	61.9	11.68	11.13	0.11	6	2000
	6-8	0.85	0.163		55.2				8	1997
	8-10	0.85	0.163	0.72	49.7	8.97	8.87	0.26	10	1994
	10-12	0.83	0.196		41.9				12	1991
	12-14	0.86	0.154	0.56	54.6	8.57	8.27	0.01	14	1989
	14-16	0.88	0.128		56.7				16	1986
	16-18	0.89	0.119	0.47	52.3	6.49	6.79	0.40	18	1983
	18-20	0.89	0.114		53.2				20	1980
	20-22	0.89	0.115	0.55	46.9	6.11	5.74	0.58	22	1978
	22-24	0.85	0.161		34.8				24	1975
	24-26	0.84	0.178	0.80	31.9	4.63	3.90	1.78	26	1972
	26-28	0.81	0.220		29.0				28	1969
	28-30	0.79	0.237	0.99	30.8	3.91	3.22	4.43	30	1967
	30-32	0.78	0.259		29.0				32	1964
	32-34	0.77	0.265	1.07	27.6	2.54	1.97	2.08	34	1961
	34-36	0.77	0.272		25.7				36	1958
	36-38	0.78	0.256	1.03	29.1	2.60	1.89	0.70	38	1956
	38-40	0.78	0.258		29.1				40	1953
	40-42	0.78	0.259	1.03	30.5	2.40	1.61	0.32	42	1950
	42-44	0.78	0.253		32.0				44	1947
	44-46	0.82	0.206	0.77	45.3	1.52	1.02	0.11	46	1945
	46-48	0.84	0.181		55.6				48	1942
	48-50	0.84	0.177	0.69	59.3	0.84	1.04	-0.10	50	1939
	50-52	0.85	0.170		61.6				52	1936
	52-54	0.85	0.170	0.67	61.2	0.71	0.36	0.23	54	1934
	54-56	0.85	0.162		65.8				56	1931
	56-58	0.85	0.160	0.64	68.2	0.53	-0.06	-0.04	58	1928
	58-60	0.86	0.158		68.2				60	1925
	60-62	0.86	0.155	0.61	71.3	0.65	0.73	-0.08	62	1922
	62-64	0.86	0.152		71.1				64	1920
	64-66	0.86	0.154	0.60	70.6	-0.05	-0.13	0.01	66	1917
	66-68	0.87	0.145		70.7				68	1914
	68-70	0.87	0.147	0.56	69.4	1.04	1.24	-0.10	70	1911
	70-72	0.88	0.135		67.0				72	1909
	72-74	0.88	0.124	0.51	64.6	-0.07	-0.38	0.01	74	1906

74-76	0.88	0.133		55.4				76	1903
76-78	0.87	0.143	0.57	51.9	0.88	0.14	-0.10	78	1900
78-80	0.87	0.142		51.4				80	1898
80-82	0.87	0.143	0.59	51.8	0.62	0.68	-0.07	82	1895
82-84	0.86	0.151		53.6				84	1892
84-86	0.86	0.157	0.63	53.1	0.55	0.43	0.06	86	1889
86-88	0.85	0.160		53.7				88	1887
88-90	0.85	0.169	0.68	51.4	0.77	0.41	0.02	90	1884
90-92	0.85	0.169		52.2				92	1881
92-94	0.84	0.182	0.73	49.3	0.07	-0.24	0.16	94	1878

Based on sedimentation Rate (xsPb-210 CA) = 0.74 cm/yr

**Table 4. Bulk sediment properties and radioisotope data for MK-3.**

Chem ID	Interval	Water Fraction	Dry Bulk Density (g/cm <sup>3</sup> )	Accumulated Mass (g/cm <sup>2</sup> )	LOI (%)	Total <sup>210</sup> Pb (dpm/g)	Excess <sup>210</sup> Pb (dpm/g)	<sup>137</sup> Cs (dpm/g)	z (cm)	Age Model
	0-2	0.74	0.304	1.12	33.9	11.85	11.44	0.29	2	2004
	2-4	0.78	0.256		46.1				4	2000
	4-6	0.73	0.321	0.64	40.3	8.67	7.51	0.23	6	1996
	6-8	0.77	0.270	0.54	44.0	7.11	6.73	0.46	8	1993
	8-10	0.82	0.203	0.84	52.0	6.18	5.62	1.12	10	1989
	10-12	0.81	0.218		48.3				12	1985
	12-14	0.79	0.239	0.88	38.3	6.33	5.75	3.61	14	1981
	14-16	0.82	0.203		35.1				16	1977
	16-18	0.83	0.191	0.78	33.5	4.22	3.74	4.70	18	1973
	18-20	0.82	0.197		35.3				20	1970
	20-22	0.83	0.186	0.71	37.9	4.27	4.24	2.04	22	1966
	22-24	0.85	0.168		37.5				24	1962
	24-26	0.86	0.158	0.65	36.3	3.92	3.44	0.21	26	1958
	26-28	0.85	0.169		34.4				28	1954
	28-30	0.81	0.220	0.93	32.1	2.44	1.68	0.21	30	1950
	30-32	0.79	0.247		27.3				32	1946
	32-34	0.81	0.221	0.93	32.0	2.40	1.43	0.08	34	1943
	34-36	0.79	0.244		29.5				36	1939
	36-38	0.81	0.216	0.82	26.4	1.36	0.72	-0.12	38	1935
	38-40	0.83	0.196		34.3				40	1931
	40-42	0.85	0.168	0.70	33.9	1.23	1.03	-0.14	42	1927
	42-44	0.84	0.181		38.1				44	1923
	44-46	0.77	0.269	1.07	29.1	1.13	0.58	-0.04	46	1920
	46-48	0.77	0.267		37.0				48	1916
	48-50	0.77	0.262	0.97	27.2	1.60	0.77	-0.08	50	1912
	50-52	0.80	0.225		30.4				52	1908
	52-54	0.83	0.196		29.2					
	54-56	0.80	0.223		28.4					
	56-58	0.74	0.311		24.6					
	58-60	0.68	0.400		25.0					
	60-62	0.68	0.397		25.0					
	62-64	0.72	0.343		30.7					
	64-66	0.75	0.290		35.6					
	66-68	0.75	0.292		40.7					
	68-70	0.75	0.295		37.9					
	70-72	0.74	0.311		37.5					
	72-74	0.75	0.296		36.1					

74-76	0.76	0.278	39.3
76-78	0.77	0.273	38.1
78-80	0.78	0.256	37.8
80-82	0.77	0.266	35.5
82-84	0.76	0.288	30.8
84-86	0.68	0.401	21.2
86-88	0.67	0.415	17.7
88-90	0.64	0.460	16.6
90-92	0.60	0.525	13.1
92-94	0.57	0.588	12.0
94-96	0.58	0.575	12.0
96-98	0.54	0.635	11.1

Based on sedimentation Rate (xsPb-210 CA) = 0.60 cm/yr

**Table 5. Bulk sediment properties and radioisotope data for MK-4.**

Chem ID	Interval	Water Fraction	Dry Bulk Density (g/cm <sup>3</sup> )	Accumulated Mass (g/cm <sup>2</sup> )	LOI (%)	Total <sup>210</sup> Pb (dpm/g)	Excess <sup>210</sup> Pb (dpm/g)	<sup>137</sup> Cs (dpm/g)	z (cm)	Age Model
	0-2	0.58	0.570	1.14	27.0	9.93	8.84	0.32	2	2002
	2-4	0.60	0.535	1.07	17.0	10.08	9.02	0.17	4	1996
	4-6	0.64	0.466	0.93	37.8	8.46	7.39	0.28	6	1989
	6-8	0.63	0.479	0.96	22.4	6.25	5.45	0.85	8	1983
	8-10	0.66	0.436	1.81	28.4	4.97	4.28	2.00	10	1977
	10-12	0.64	0.467		20.2				12	1971
	12-14	0.69	0.383	0.77	25.5	3.79	3.04	2.06	14	1964
	14-16	0.71	0.348	0.70	29.0	4.03	3.21	1.80	16	1958
	16-18	0.71	0.347	1.43	26.7	2.89	2.12	0.63	18	1952
	18-20	0.70	0.366		24.7				20	1946
	20-22	0.66	0.434	0.87	18.4	2.27	1.17	0.24	22	1939
	22-24	0.69	0.380	0.76	20.0	2.10	1.18	0.00	24	1933
	24-26	0.67	0.408	0.82	17.1	1.92	0.66	0.01	26	1927
	26-28	0.66	0.439	0.88	15.0	1.91	0.77	0.00	28	1921
	28-30	0.65	0.451	0.90	14.2	1.46	0.43	-0.02	30	1914
	30-32	0.65	0.455	0.91	13.7	2.24	1.22	0.04	32	1908
	32-34	0.60	0.537	1.07	12.2	1.49	0.17	0.01	34	1902
	34-36	0.58	0.566	1.13	11.7	1.31	0.31	-0.04	36	1896
	36-38	0.56	0.608	1.22	12.1	1.13	-0.23	0.03	38	1889
	38-40	0.55	0.629	1.26	11.8	1.77	0.76	-0.04	40	1883
	40-42	0.54	0.646	1.29	11.7	1.22	0.05	0.11	42	1877
	42-44	0.52	0.691	1.38	12.1	1.28	-0.10	-0.04	44	1871
	44-46	0.54	0.638	1.28	11.5	0.63	-0.51	-0.04	46	1864
	46-48	0.52	0.682	1.36	11.6	1.76	0.44	0.03	48	1858
	48-50	0.50	0.728	1.46	9.7	1.70	0.36	-0.03	50	1852
	50-52	0.48	0.763		9.6					
	52-54	0.52	0.683		10.5					
	54-56	0.57	0.592		12.8					
	56-58	0.59	0.554		12.4					
	58-60	0.60	0.526		13.9					
	60-62	0.61	0.517		11.7					
	62-64	0.61	0.514		13.4					
	64-66	0.64	0.458		13.1					
	66-68	0.62	0.503		13.0					
	68-70	0.62	0.490		12.0					
	70-72	0.62	0.493		13.0					
	72-74	0.61	0.508		11.5					

74-76	0.59	0.547	13.0
76-78	0.58	0.566	11.7
78-80	0.59	0.555	13.9
80-82	0.62	0.502	14.0
82-84	0.57	0.583	14.0
84-86	0.60	0.539	13.6
86-88	0.62	0.494	18.5
88-90	0.65	0.444	19.2
90-92	0.64	0.468	19.1
92-94	0.62	0.500	15.2
94-96	0.62	0.495	17.6

Based on sedimentation Rate (xsPb-210 CA) = 0.33 cm/yr

**Table 6. Summary data for radioisotope analysis and dating.**

Location	Core	Radioisotope Inventory		Sedimentation Rate		Mass Accumulation Rate		Depositional Flux	Focusing Factor	
		xsPb-210	Cs-137	xsPb-210 (CA)	Cs-137	xsPb-210	Cs-137	xsPb-210	xsPb-210	Cs-137
		dpm/cm <sup>2</sup>	dpm/cm <sup>2</sup>	cm/yr	cm/yr	g/cm <sup>2</sup> -yr	g/cm <sup>2</sup> -yr	dpm/cm <sup>2</sup> -yr		
Upstream	MK-1	65.80	9.38	0.74	0.71	0.20	0.19	0.80	2.35	0.45
	MK-2	47.29	10.04	0.74	0.71	0.13	0.12	0.36	1.69	0.48
	MK-3	44.81	10.03	0.60	0.44	0.14	0.10	0.45	1.60	0.48
Downstream	MK-4	53.40	9.20	0.33	0.31	0.17	0.16	0.34	1.91	0.44

xs – excess; CA – Constant activity model; Depositional flux – based on steady-state atmospheric fluxes of xsPb-210 (32 dpm/cm<sup>2</sup>-yr) and Cs-137 (21 dpm/cm<sup>2</sup>-yr)



**Table 7. Concentrations of various parameters for Core MK-1.**

<b>CHEM ID</b>	<b>Interval</b>	<b>Mid-Point</b>	<b>Solids</b>	<b>Age Model</b>	<b><math>\delta^{13}\text{C}</math></b>	<b><math>\delta^{15}\text{N}</math></b>	<b>TC</b>	<b>TN</b>	<b>TSP</b>	<b>C/N</b>
	<b>cm</b>	<b>cm</b>	<b>%</b>	<b>yr</b>	<b>‰</b>	<b>‰</b>	<b>%</b>	<b>%</b>	<b>%</b>	<b>Atomic</b>
2028	0-2	1	27.1	2006	-17.12	9.96	11.56	0.73	0.107	18.5
2030	4-6	5	28.5	2000	-17.30	9.45	10.77	0.68	0.065	18.4
2032	8-10	9	30.1	1995	-18.27	8.68	9.63	0.65	0.071	17.3
2033	10-12	11	31.7	1992	-17.53	8.63	9.18	0.62	0.075	17.2
2034	12-14	13	30.2	1990	-17.67	8.96	8.55	0.65	0.076	15.4
2035	14-16	15	26.2	1987	-17.72	9.97	9.45	0.72	0.082	15.3
2036	16-18	17	27.0	1984	-17.73	8.68	10.14	0.74	0.084	16.1
2037	18-20	19	22.1	1981	-17.58	8.84	11.59	0.74	0.077	18.4
2038	20-22	21	25.0	1979	-17.46	8.67	9.73	0.61	0.075	18.6
2039	22-24	23	23.1	1976	-17.73	7.97	10.19	0.65	0.074	18.4
2042	28-30	29	21.5	1968	-19.14	5.74	11.53	0.72	0.065	18.6
2044	32-34	33	48.1	1963	-21.14	4.88	11.90	0.66	0.065	21.2
2046	36-38	37	23.8	1957	-22.84	4.70	11.19	0.60	0.062	21.7
2048	40-42	41	24.0	1952	-26.36	3.74	11.84	0.67	0.065	20.5
2050	44-46	45	14.7	1946	-26.52	1.53	25.36	1.23	0.086	24.0
2054	52-54	53	14.4	1936	-27.12	0.59	31.18	1.54	0.080	23.6
2059	62-64	63	16.7	1922	-26.97	0.58	27.36	1.44	0.071	22.2
2064	72-74	73	19.1	1909	-25.72	0.83	25.99	1.25	0.072	24.3
2067	78-80	79	19.5	1900	-25.52	1.15	23.88	1.18	0.066	23.6
Spartina alt.	Surface		NA	NA	-13.61	9.02	10.36	1.55	NA	30.4

**Table 8. Concentrations of various parameters for Core MK-2.**

CHEM ID	Interval cm	Mid-Point cm	Solids %	Age Model yr	$\delta^{13}\text{C}$ ‰	$\delta^{15}\text{N}$ ‰	TC %	TN %	TSP %	C/N Atomic
2069	0-2	1	16.3	2006	-15.08	6.98	27.72	1.28	0.119	25.2
2071	4-6	5	16.8	2000	-16.55	6.67	25.17	1.53	0.107	19.2
2073	8-10	9	19.2	1995	-15.80	7.48	17.29	0.88	0.072	22.8
2075	12-14	13	14.2	1990	-14.84	7.29	26.33	1.31	0.080	23.4
2077	16-18	17	12.2	1984	-14.87	6.34	21.35	0.94	0.063	26.5
2079	20-22	21	12.4	1979	-15.09	6.71	21.12	0.95	0.059	26.0
2081	24-26	25	17.4	1973	-15.97	5.57	12.73	0.64	0.061	23.0
2083	28-30	29	20.6	1968	-16.08	5.21	12.63	0.58	0.057	25.4
2085	32-34	33	22.2	1963	-18.96	4.20	11.73	0.58	0.058	23.4
2087	36-38	37	21.8	1957	-21.71	3.00	12.40	0.65	0.058	22.1
2090	42-44	43	18.8	1949	-26.51	0.56	25.70	1.22	0.065	24.5
2094	50-52	51	15.1	1938	-25.84	0.03	32.14	1.69	0.079	22.2
2099	60-62	61	15.4	1925	-24.72	-0.12	34.33	1.61	0.065	24.8
2106	74-76	75	12.3	1906	-23.35	0.13	28.39	1.29	0.070	25.6
2113	88-90	89	16.6	1887	-23.35	0.55	23.20	1.05	0.064	25.8
Spartina alt.	Surface		NA	NA	-12.71	3.79	48.53	0.79	NA	71.7

Concentrations on a dry weight basis. NA- Not analyzed.

**Table 9. Concentrations of various parameters for Core MK-3.**

<b>CHEM ID</b>	<b>Interval cm</b>	<b>Mid-Point cm</b>	<b>Solids %</b>	<b>Age Model yr</b>	<b><math>\delta^{13}\text{C}</math> ‰</b>	<b><math>\delta^{15}\text{N}</math> ‰</b>	<b>TC %</b>	<b>TN %</b>	<b>TSP %</b>	<b>C/N Atomic</b>
2116	0-2	1	26.51	2005	-15.93	1.15	12.69	0.69	0.087	21.5
2118	4-6	5	29.43	1999	-15.12	0.94	14.73	0.53	0.058	32.4
2120	8-10	9	21.25	1992	-14.19	1.41	22.21	0.70	0.045	36.8
2122	12-14	13	22.88	1985	-14.21	0.03	15.59	0.63	0.071	28.9
2123	14-16	15	18.10	1982	-14.14	0.81	16.66	0.63	0.060	31.0
2124	16-18	17	18.34	1979	-14.47	0.15	14.88	0.62	0.069	27.9
2125	18-20	19	16.32	1975	-13.99	0.61	16.48	0.61	0.054	31.8
2126	20-22	21	16.47	1972	-14.21	0.34	16.12	0.60	0.054	31.4
2128	24-26	25	13.35	1965	-13.14	0.68	24.41	0.71	0.051	40.3
2130	28-30	29	19.58	1959	-14.62	0.23	12.10	0.56	0.120	25.3
2132	32-34	33	20.35	1952	-14.41	0.06	12.80	0.48	0.049	31.4
2134	36-38	37	20.68	1945	-14.85	0.38	10.93	0.43	0.054	29.7
2136	40-42	41	14.84	1939	-15.42	0.41	15.05	0.62	0.043	28.2
2140	48-50	49	22.94	1925	-14.99	0.65	10.54	0.44	0.051	28.2
2145	58-60	59	31.26	1909	-14.70	0.39	10.81	0.48	0.044	26.2
2151	70-72	71	25.97	1889	-16.20	0.00	3.36	0.21	0.058	19.0
2161	90-92	91	46.84	1855	-19.69	0.02	15.62	0.85	0.042	21.4
Spartina alt.	Surface		NA	NA	-12.74	3.74	46.57	0.71	NZ	76.5

Concentrations on a dry weight basis. NA- Not analyzed.

**Table 10. Concentrations of various parameters for Core MK-4.**

CHEM ID	Interval	Mid-Point	Solids	Age Model	$\delta^{13}\text{C}$	$\delta^{15}\text{N}$	TC	TN	TSP	C/N
	cm	cm	%	yr	‰	‰	%	%	%	Atomic
2165	0-2	1	44.1	2003	-15.28	3.34	14.12	0.54	0.157	30.4
2167	4-6	5	37.9	1991	-16.08	4.65	7.37	0.48	0.205	18.1
2169	8-10	9	38.3	1979	-16.41	4.65	6.77	0.43	0.199	18.6
2170	10-12	11	31.4	1973	-16.77	6.11	5.34	0.38	0.069	16.5
2171	12-14	13	34.9	1967	-16.14	3.75	7.05	0.45	0.069	18.3
2172	14-16	15	33.2	1961	-15.81	3.22	8.48	0.42	0.063	23.4
2173	16-18	17	30.8	1954	-15.75	2.61	8.06	0.48	0.070	19.5
2174	18-20	19	30.4	1948	-15.69	2.24	9.00	0.49	0.059	21.5
2175	20-22	21	39.2	1942	-15.56	2.43	5.55	0.29	0.054	22.3
2176	22-24	23	36.5	1936	-15.95	1.99	5.91	0.33	0.058	21.2
2179	28-30	29	32.9	1918	-15.83	1.86	6.25	0.33	0.049	22.3
2181	32-34	33	45.4	1906	-16.66	2.82	3.79	0.28	0.050	15.8
2183	36-38	37	45.5	1894	-15.72	3.10	3.73	0.29	0.048	14.9
2185	40-42	41	46.3	1882	-15.04	2.66	4.41	0.31	0.048	16.5
2187	44-46	45	48.1	1870	-15.91	3.06	2.74	0.22	0.052	14.6
2189	48-50	49	49.8	1857	-16.64	3.74	2.32	0.21	0.049	13.0
2191	52-54	53	51.6	1845	-15.78	3.21	3.12	0.24	0.049	15.3
2193	56-58	57	40.5	1833	-14.94	2.03	5.35	0.33	0.053	18.8
2199	68-70	69	40.5	1797	-16.01	1.79	4.17	0.25	0.046	19.5
2203	76-78	77	41.4	1773	-15.75	0.61	4.52	0.31	0.046	17.3
2206	82-84	83	41.1	1754	-15.65	0.53	5.35	0.34	0.047	18.2
2209	88-90	89	37.5	1736	-14.56	0.86	7.71	0.44	0.051	20.2
2212	94-96	95	39.2	1718	-14.24	1.64	5.45	0.31	0.048	20.6
Spartina alt.	Surface				-13.23	4.17	45.23	0.70		75.4

Concentrations on a dry weight basis. NA- Not analyzed.

**Table 11. Diatom Metrics determined from species identification: MK-1.**

<b>Core ID/ Depth Interval (cm)</b>	<b>Mid-Depth (cm)</b>	<b>Eutrophentic</b>	<b>Meso/ eurotrophentic</b>	<b>Mesotrophentic</b>	<b>Oligotrophentic</b>	<b>Oligo/ mesotrophentic</b>	<b>Unknow</b>
0-2	1	38.0	3.3	0.0	0.0	0.0	57.8
4-6	5	48.0	1.8	0.5	0.3	0.0	49.0
8-10	9	45.5	1.3	0.0	0.0	0.0	50.8
12-14	13	44.0	1.5	0.0	0.8	0.8	51.3
16-18	17	39.5	4.5	0.0	0.0	0.0	55.0
20-22	21	37.5	7.8	0.0	0.0	0.0	53.5
22-24	23	37.3	10.3	0.0	1.3	0.0	51.3
28-30	29	54.3	4.0	0.8	0.3	0.0	40.8
32-34	33	61.3	7.8	0.0	2.0	0.0	29.0
36-38	37	68.3	5.3	0.0	0.8	0.0	24.8
44-46	45	12.8	9.0	2.0	51.8	1.0	22.5
52-54	53	9.3	7.3	0.8	70.3	0.5	12.0
62-64	63	18.8	11.5	4.3	31.5	5.0	29.0
72-74	73	24.0	10.5	8.5	20.5	6.5	29.3
78-80	79	22.5	9.8	7.5	9.8	8.0	39.8

Metrics based on van Dam et al. (1994)

**Table 12. Diatom Metrics determined from species identification: MK-2.**

Core ID/ Depth Interval (cm)	Mid-Depth (cm)	Eutrophentic	Meso/ eurotrophentic	Mesotrophentic	Oligotrophentic	Oligo/ mesotrophentic	Unknow
0-2	1	21.8	4.3	2.5	0.0	0.0	70.3
4-6	5	20.3	14.0	1.0	3.8	0.0	61.0
8-10	9	41.8	4.8	0.5	2.3	0.5	49.8
12-14	13	27.5	16.3	0.0	0.0	0.0	56.3
16-18	17	26.0	29.0	0.3	0.0	0.0	44.8
20-22	21	26.8	12.3	1.0	0.0	0.3	59.3
24-26	25	53.0	3.3	3.5	0.3	0.0	40.0
28-30	29	59.5	1.3	3.0	0.0	0.5	34.5
32-34	33	53.5	1.3	3.0	0.8	2.3	39.3
36-38	37	44.5	6.8	0.5	9.0	0.5	38.8
42-44	43	15.0	7.0	1.5	43.5	1.5	31.5
50-52	53	3.0	12.5	0.3	72.5	0.0	11.8
60-62	63	27.5	2.3	3.5	34.5	1.3	31.0
88-90	89	21.3	7.5	2.5	6.0	1.8	60.8

Metrics based on van Dam et al. (1994)

**Table 13. Diatom Metrics determined from species identification: MK-3.**

Core ID/ Depth Interval (cm)	Mid-Depth (cm)	Eutrophentic	Meso/ eurotrophentic	Mesotrophentic	Oligotrophentic	Oligo/ mesotrophentic	Unknown
0-2	1	37.5	0.3	1.3	0.0	0.0	60.0
4-6	5	44.5	0.5	0.5	0.0	0.0	53.5
8-10	9	65.8	0.5	0.0	0.0	0.0	32.8
12-14	13	62.8	1.8	0.5	0.0	0.0	35.0
14-16	15	58.0	2.8	0.0	0.0	0.5	37.8
16-18	17	51.5	2.8	0.3	0.0	0.8	44.8
20-22	21	37.8	6.3	0.0	0.0	0.0	56.0
24-26	25	35.0	1.8	1.0	0.0	0.0	62.0
28-30	29	24.0	0.8	0.0	0.0	1.8	72.5
32-34	33	35.3	4.3	1.8	0.0	1.5	56.3
36-38	37	23.3	5.3	4.5	0.0	0.0	67.0
40-42	41	30.3	4.3	9.0	0.0	3.5	52.5
48-50	49	22.3	8.8	4.8	0.0	1.3	63.0
58-60	59	25.0	15.5	2.0	0.0	2.3	55.3
70-72	71	26.8	10.3	3.0	2.0	1.5	55.0
90-92	91	39.0	2.0	1.3	0.0	0.5	57.3

Metrics based on van Dam et al. (1994)

**Table 14. Diatom Metrics determined from species identification: MK-4.**

<b>Core ID/ Depth Interval (cm)</b>	<b>Mid-Depth (cm)</b>	<b>Eutrophentic</b>	<b>Meso/ eutrophentic</b>	<b>Mesotrophentic</b>	<b>Oligotrophentic</b>	<b>Oligo/ mesotrophentic</b>	<b>Unknow</b>
0-2	1	18.0	0.8	0.0	0.0	0.0	80.0
4-6	5	27.6	0.5	0.0	0.3	0.0	70.7
8-10	9	27.9	1.7	1.2	0.5	0.0	68.7
10-12	13	34.0	0.0	0.0	0.3	2.0	63.7
12-14	15	25.7	0.0	0.3	0.3	0.0	73.7
16-18	17	28.0	1.0	0.7	0.0	1.3	69.0
20-22	21	23.8	0.3	0.0	0.0	0.9	74.9
24-26	25	27.4	0.3	0.7	0.3	1.0	70.4
28-30	29	24.7	0.3	0.0	0.0	5.7	69.3
40-42	43	17.7	0.0	1.3	0.0	0.0	81.1
56-58	57	25.5	0.0	0.7	0.0	1.0	72.9

Metrics based on van Dam et al. (1994)



## Figures

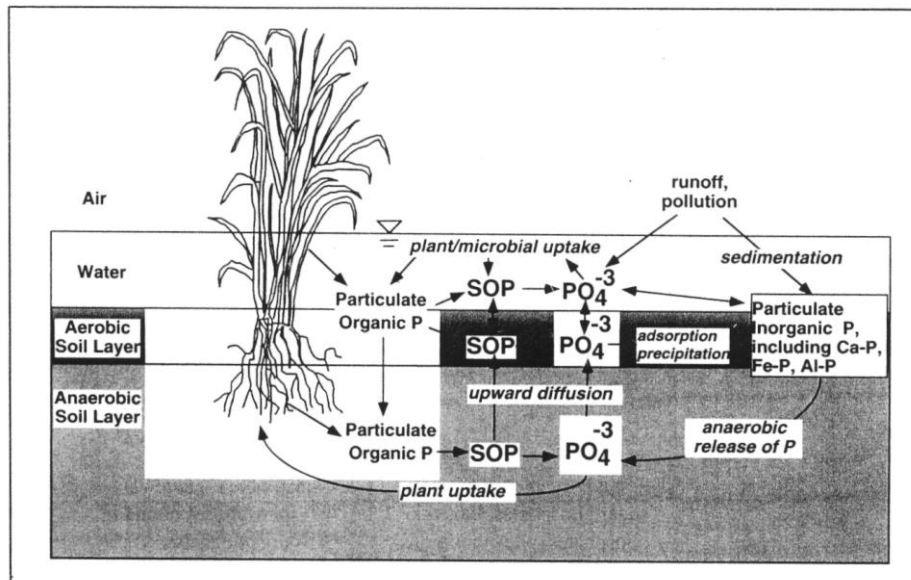
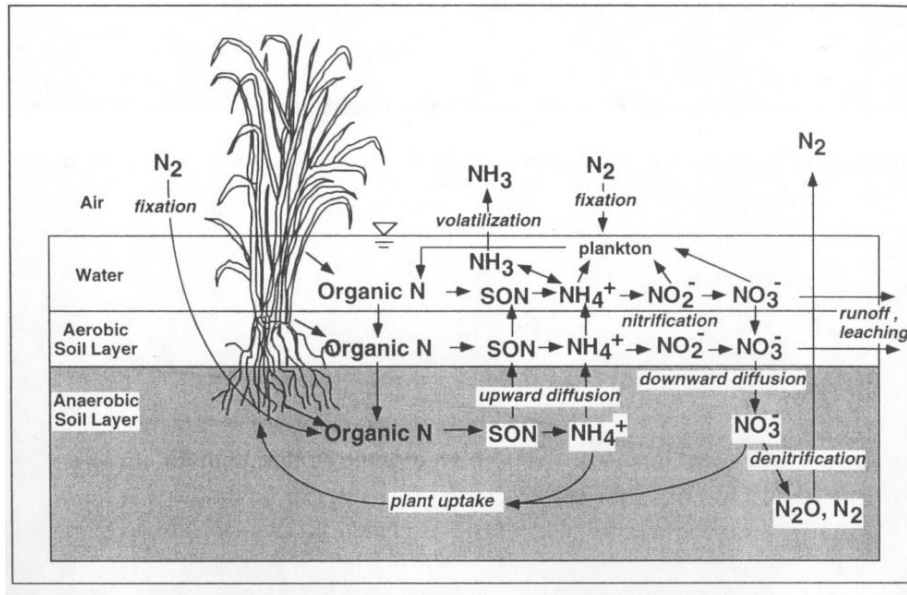


Figure 1a,b. Generalized schematic of nitrogen and phosphorus cycling in wetlands. SOP – soluble organic phosphorus. In marine sediments, dissolved sulfide (from sulfate reduction) can bind reduced iron, allowing for greater movement of porewater P from the sediments to the overlying water. (Images taken from Mitch and Gosselink, 1993)



Figure 2. Coring locations within the tidal Murderkill River system. Key: The Kent County WWTP is located up the tidal creek near MK-2(A,B).



Figure 3. Tripod and pulley system used to retrieve push-piston cores the Murderkill River. Upper picture is from the upper tidal river (MK-1) while the lower picture is from MK-4, near the tidal inlet and the Delaware Estuary.

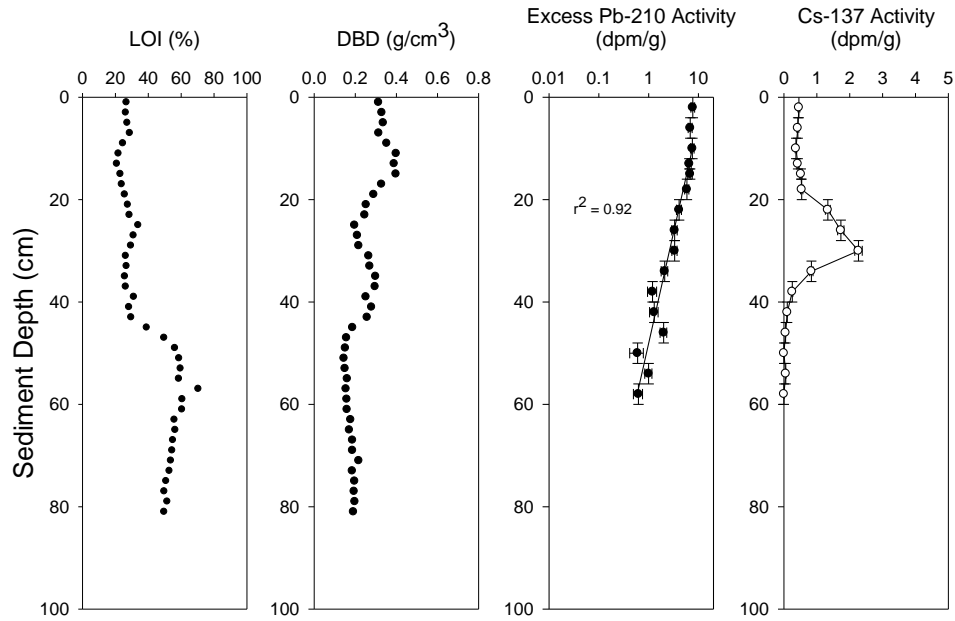


Figure 4. Geochronology for the MK-1B marsh using excess  $^{210}\text{Pb}$  and transient fallout  $^{137}\text{Cs}$ . The radionuclides give comparable sedimentation rates of 0.74 (constant activity model) and 0.71 cm/yr, respectively. The first occurrence of  $^{137}\text{Cs}$  at ~48 cm is assumed concordant with ca. 1954.

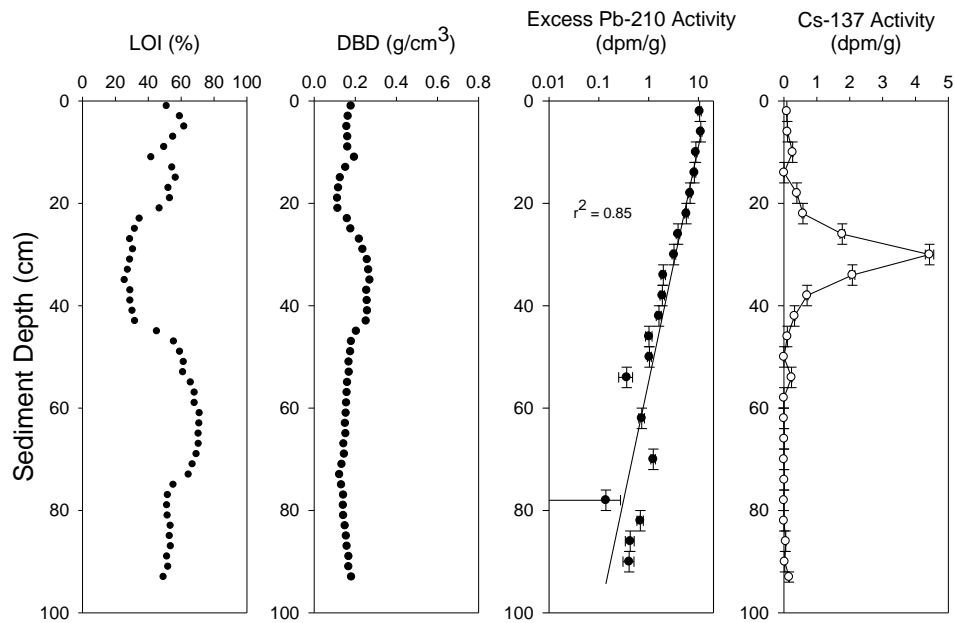


Figure 5. Geochronology for the MK-2B using excess  $^{210}\text{Pb}$  and transient fallout  $^{137}\text{Cs}$ . The radionuclides give comparable sedimentation rates of 0.74 (constant activity model) and 0.71 cm/yr, respectively. The first occurrence of  $^{137}\text{Cs}$  at ~48 cm is assumed concordant with ca. 1954.

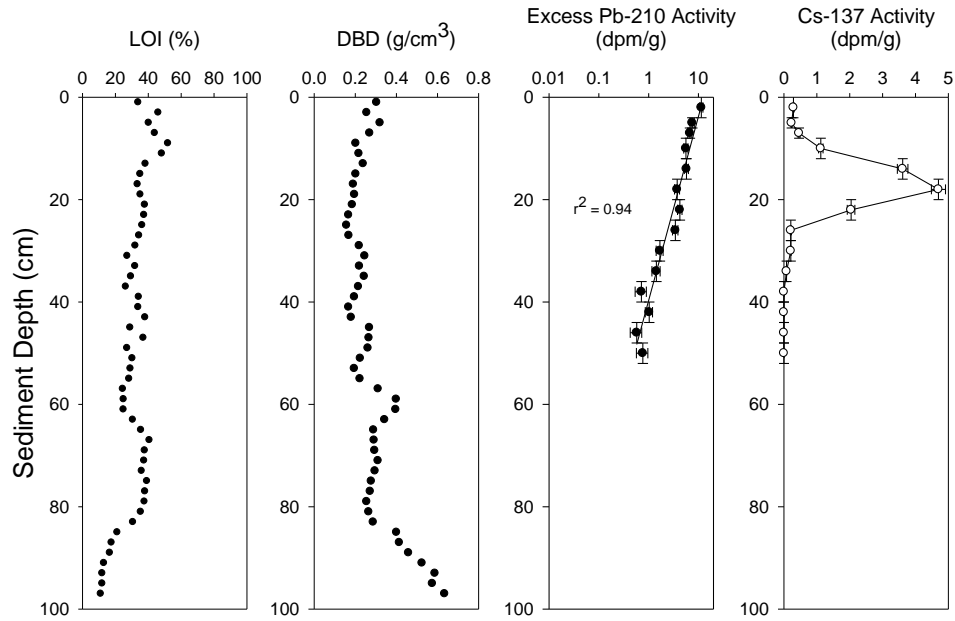


Figure 6. Geochronology for the MK-3B using excess  $^{210}\text{Pb}$  and transient fallout  $^{137}\text{Cs}$ . The radionuclides give slightly different sedimentation rates of 0.60 (constant activity model) and 0.44 cm/yr, respectively. The first occurrence of  $^{137}\text{Cs}$  at ~36 cm is assumed concordant with ca. 1954.

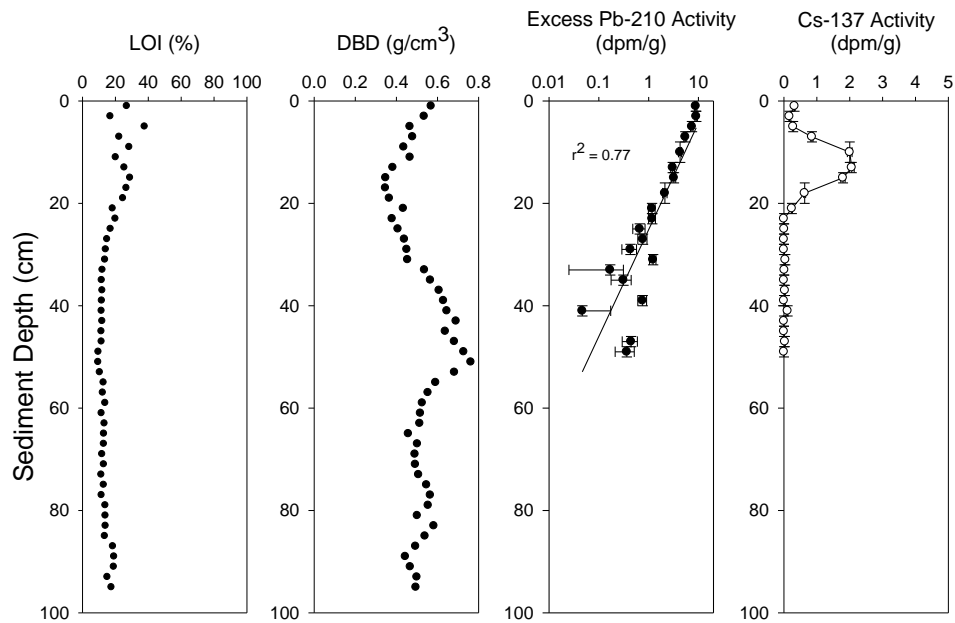


Figure 7. Geochronology for the MK-4B using excess  $^{210}\text{Pb}$  and transient fallout  $^{137}\text{Cs}$ . The radionuclides give identical sedimentation rates of 0.33-0.31 cm/yr, respectively using the constant activity model for  $^{210}\text{Pb}$ . The first occurrence of  $^{137}\text{Cs}$  at ~22 cm is assumed concordant with ca. 1954.

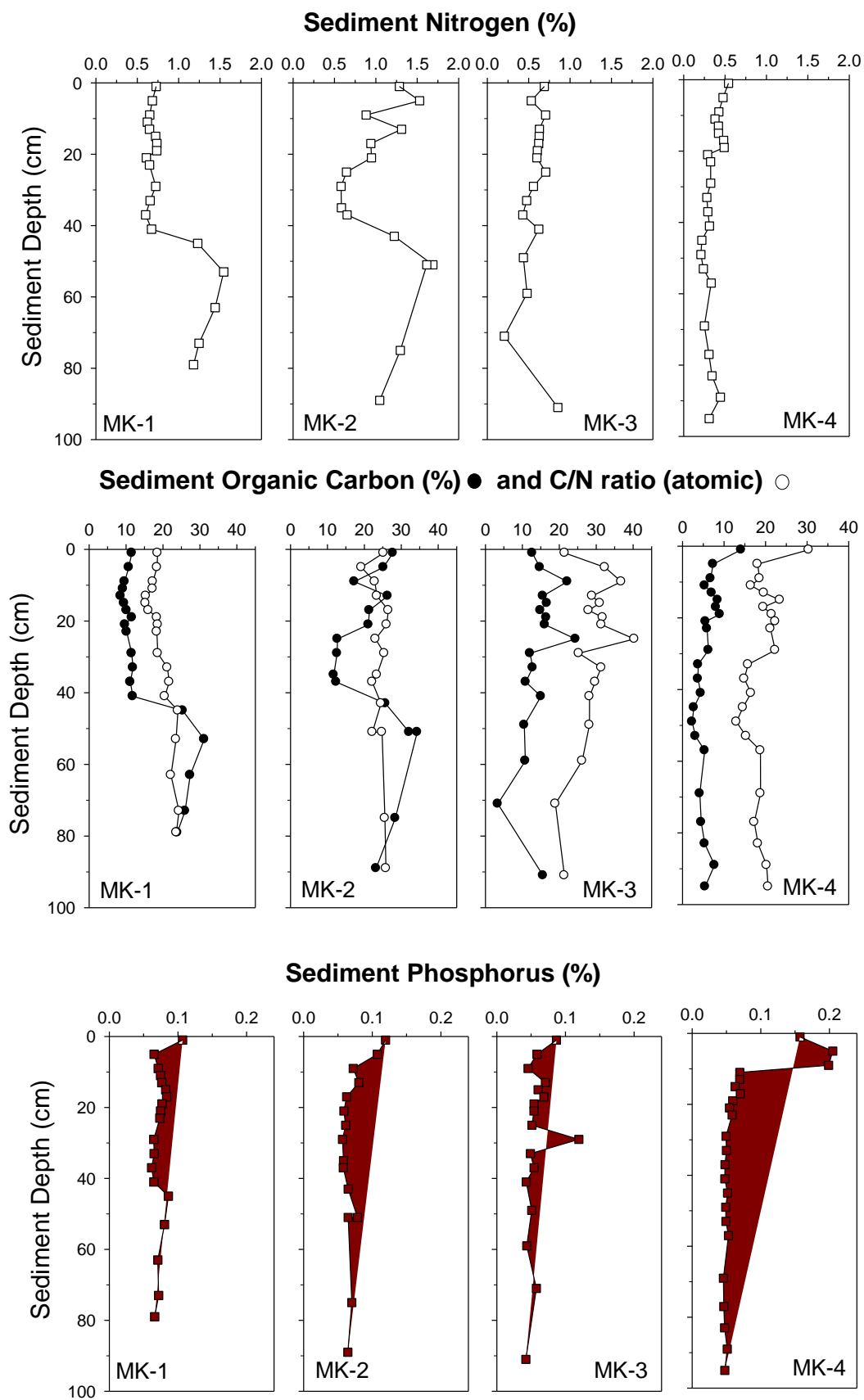


Figure 8. Sediment organic carbon, total nitrogen, C/N and sediment phosphorus distribution with depth in the marshes of the Murderkill River.

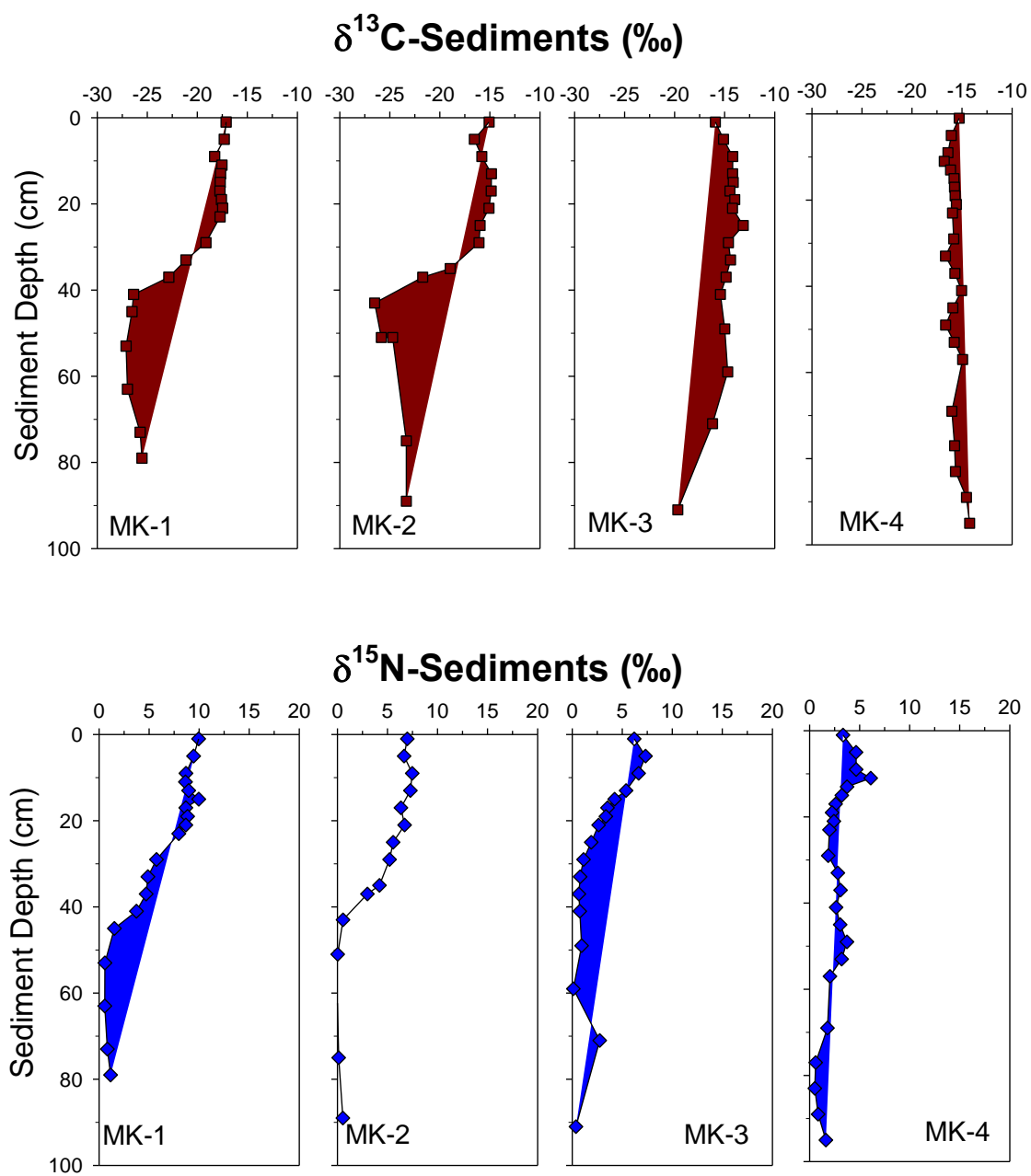


Figure 9. Depth distribution of the isotopic composition of sediment N ( $\delta^{15}\text{N}$ ) and C ( $\delta^{13}\text{C}$ ) from the tidal Murderkill River.



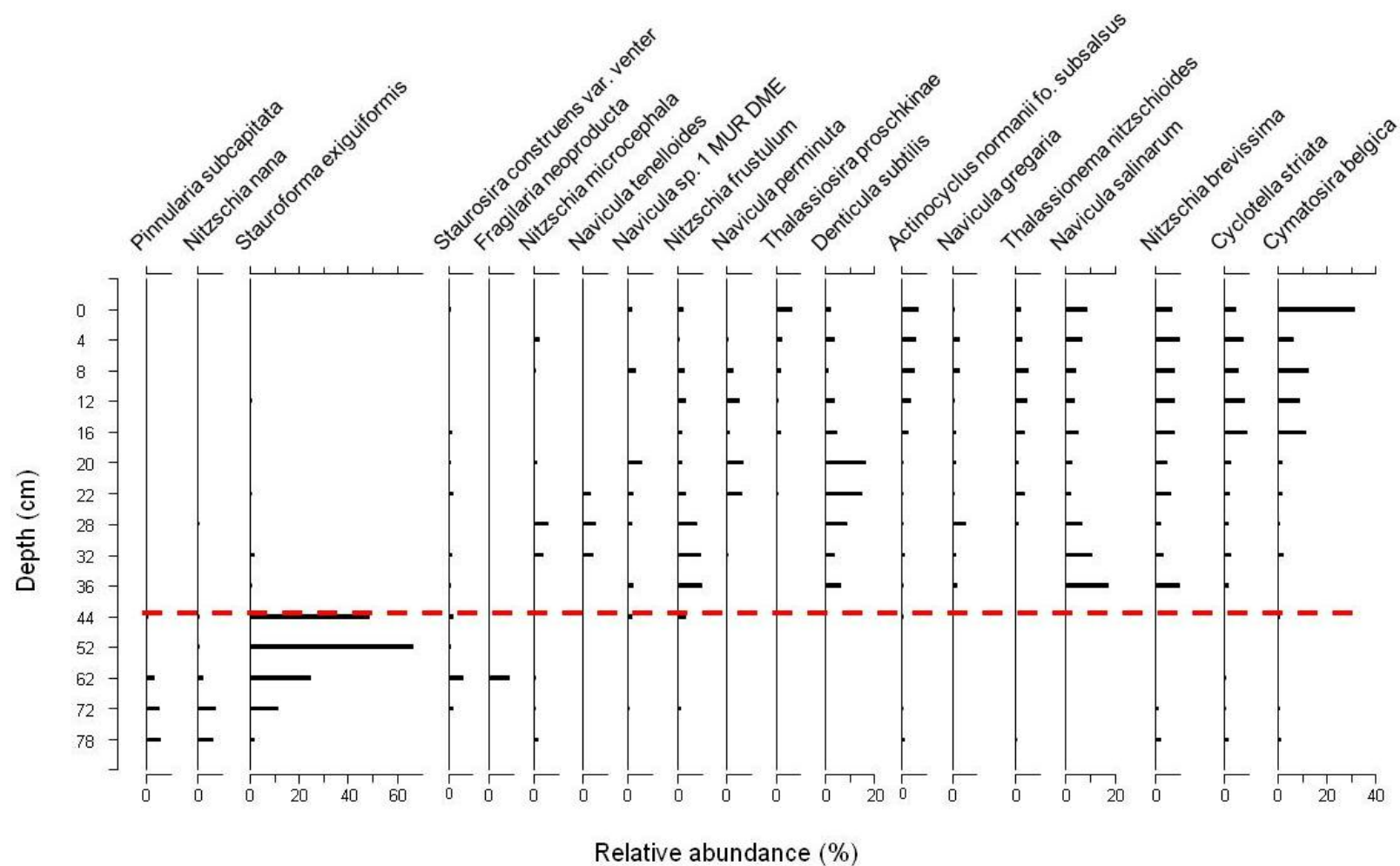


Figure 10. Stratigraphic diagram of diatom species with relative abundances > 5% in at least a sample from core MK-1. Dashed line represents the major shift in diatom assemblages from freshwater *S. exiguiiformis* dominant to marine-brackish dominant coastal species.

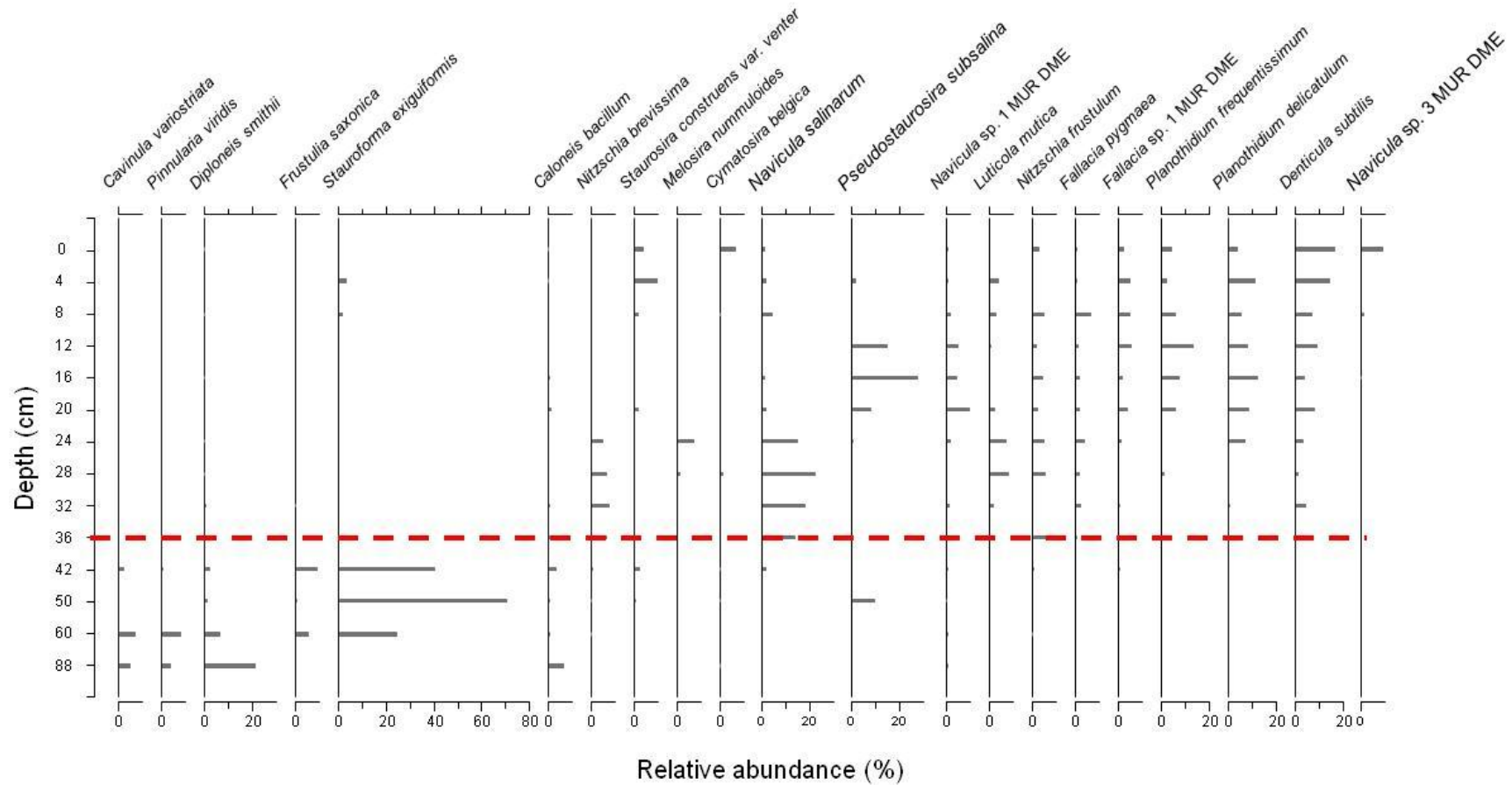


Figure 11. Stratigraphic diagram of diatom species with relative abundances > 5% in at least a sample from core MK-2. Dashed line represents the major shift in diatom assemblages from freshwater *S. exiguiformis* dominant to marine-brackish dominant coastal species.

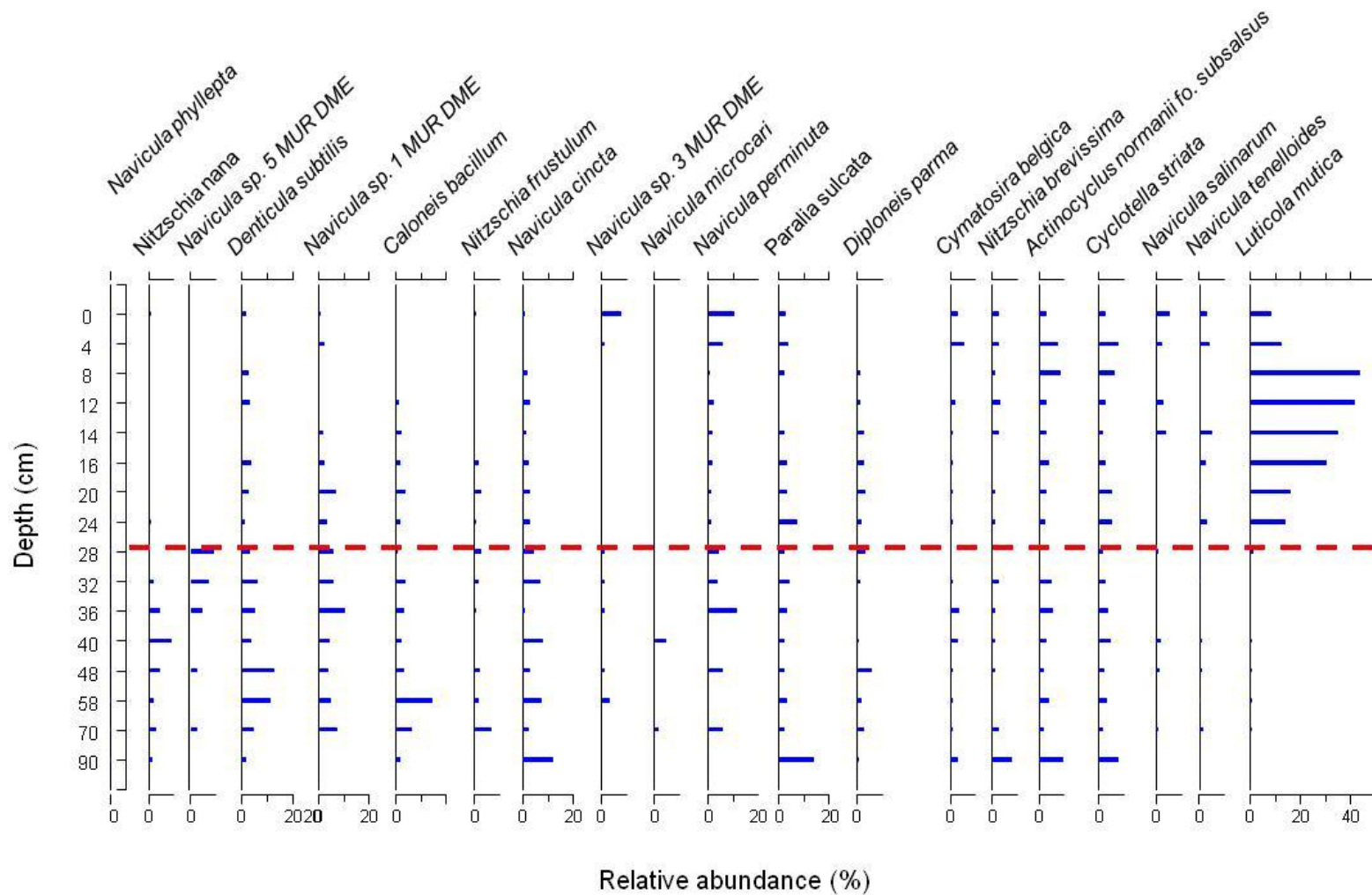


Figure 12. Stratigraphic diagram of diatom species with relative abundances > 5% in at least a sample from core MK-3. Dashed line represents the major shift in diatom assemblages from diverse, mixed marine and eutrophic freshwater species to an assemblage with abundant subaerial *Luticola mutica*.

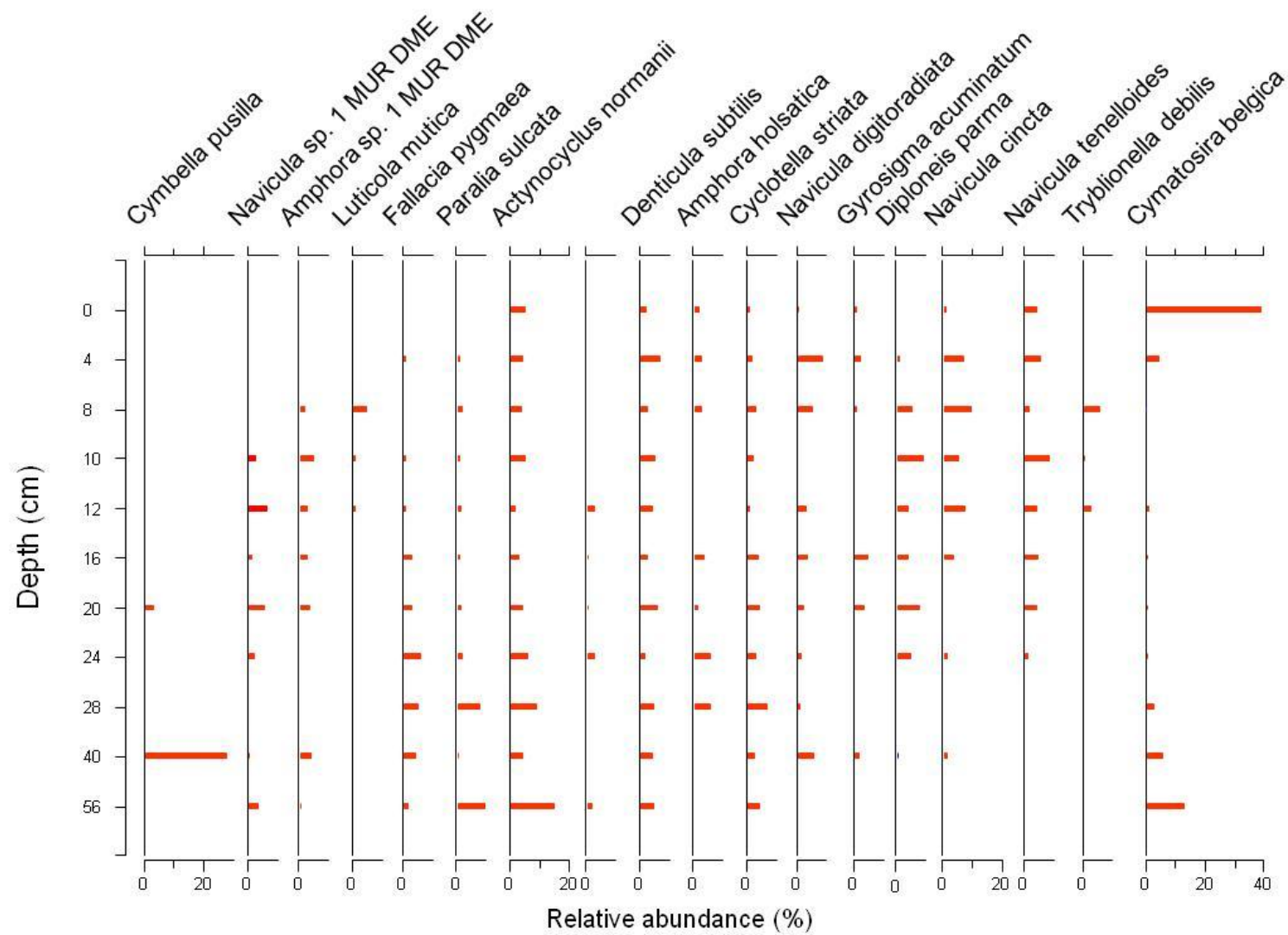


Figure 13. Stratigraphic diagram of diatom species with relative abundances > 5% in at least a sample from core MK-4.

## % Diatom Metric (van Dam et al, 1994)

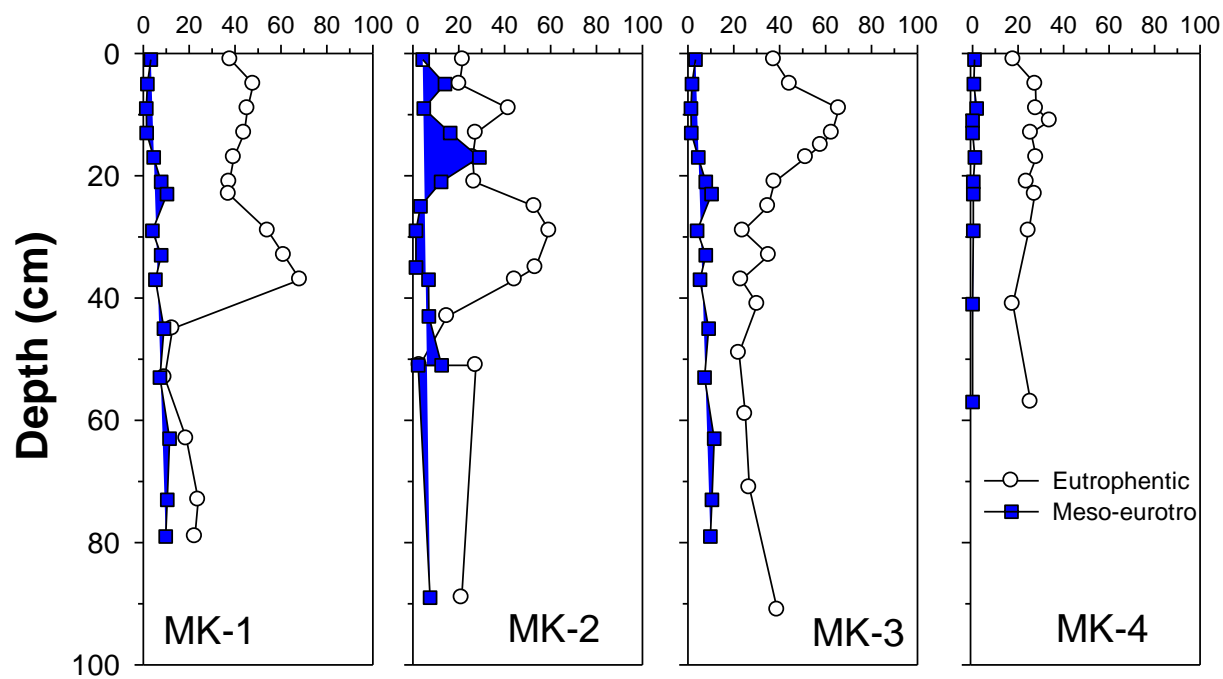


Figure 14. Diatom metrics for the cores of the tidal Christina River using the van Dam et al. (1994).

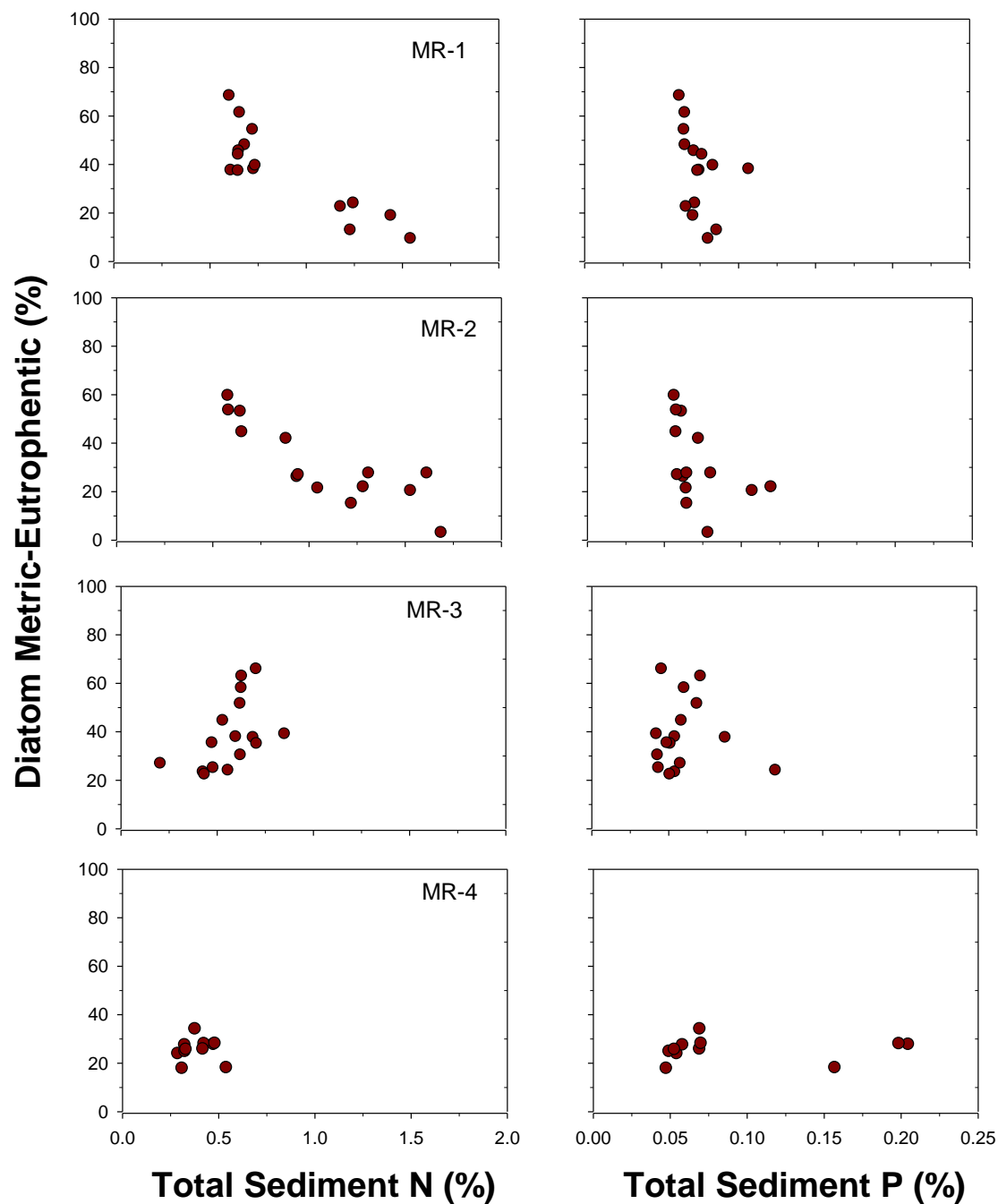


Figure 15. Relationship between total sediment N and P, and the diatom metric for eutrophic species in each core.

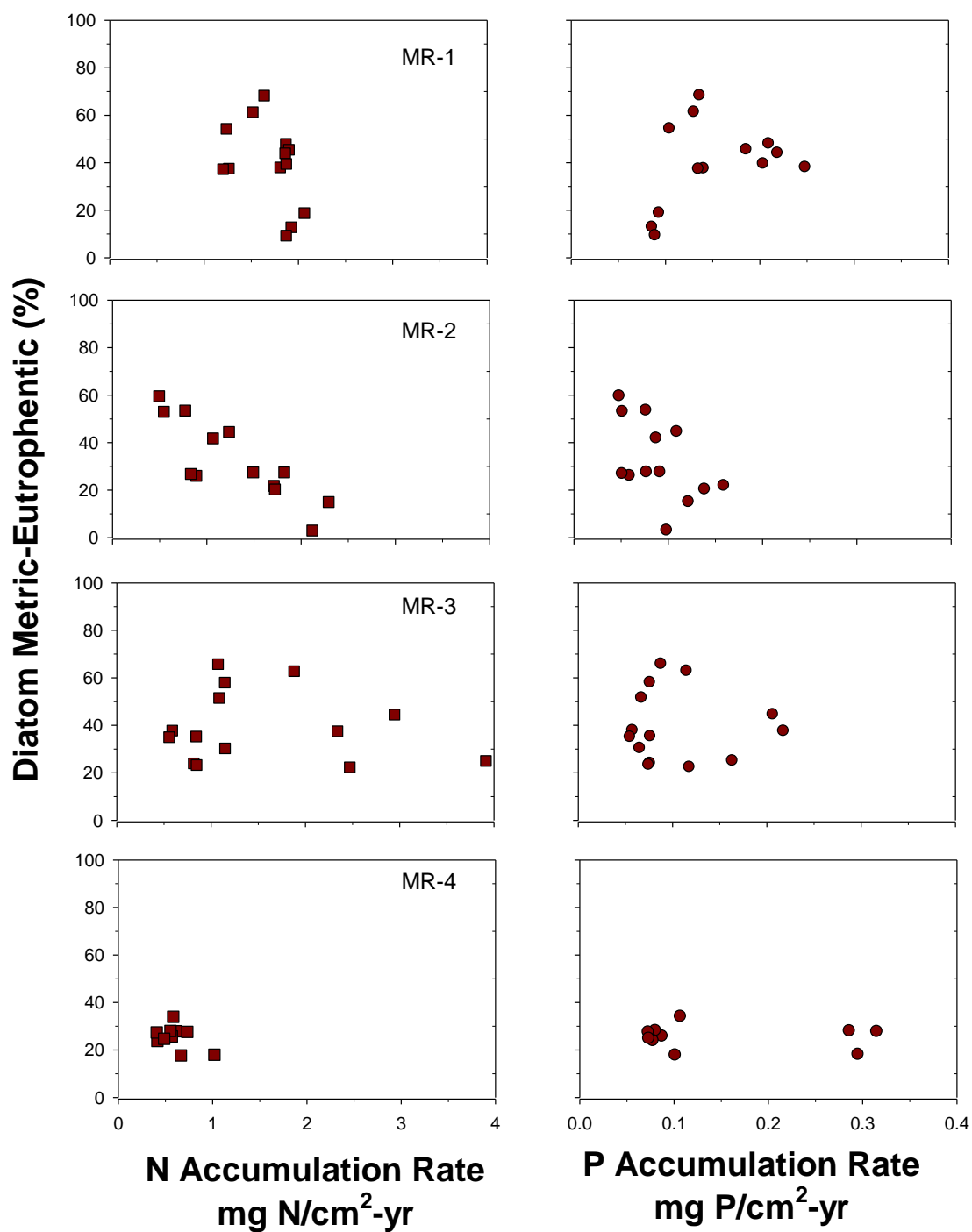


Figure 16. Relationship between the accumulation rate of sediment N and P and the diatom metric for eutrophentic species in each core.

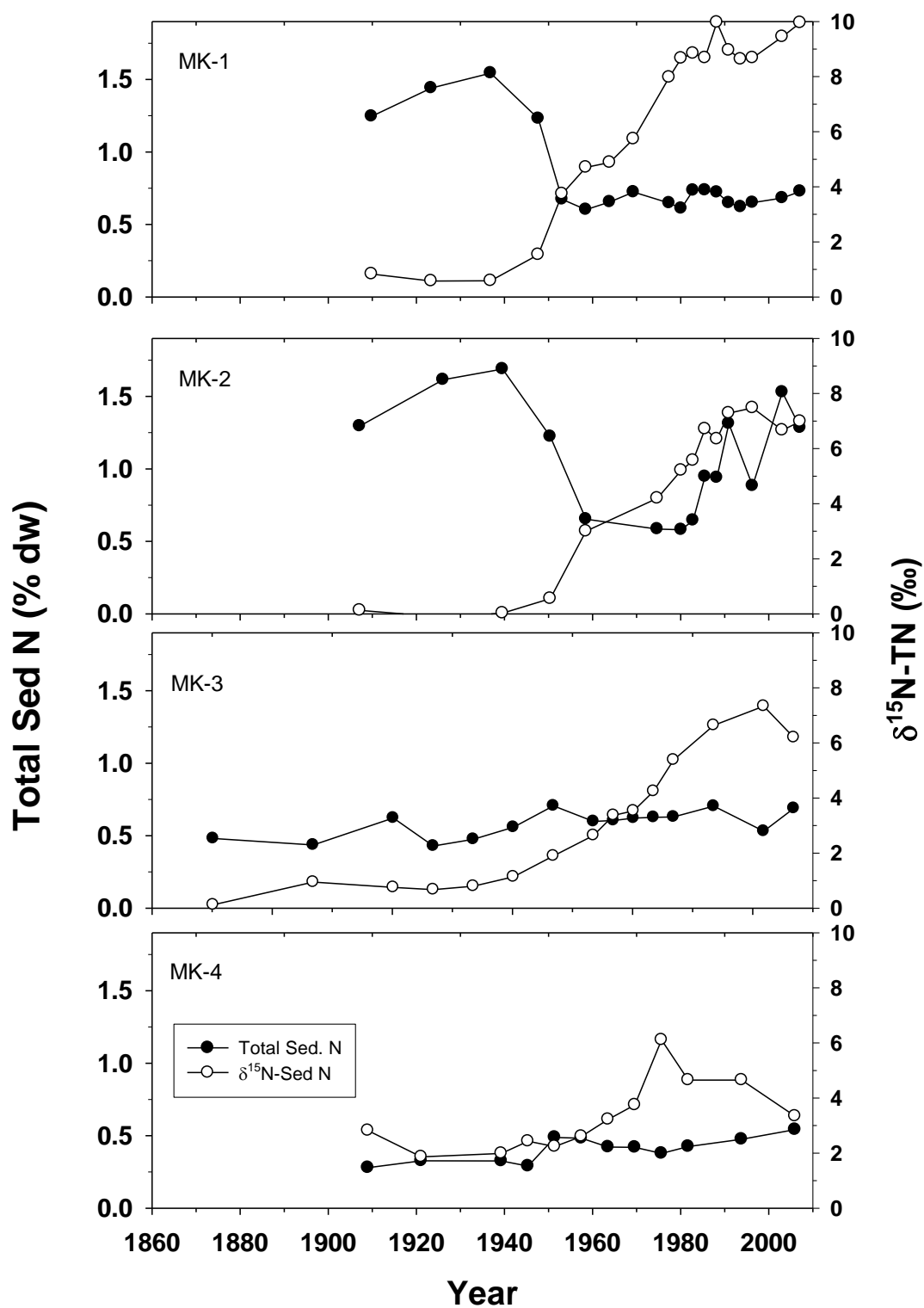


Figure 17. Concentrations of total sediment nitrogen (TN) and the nitrogen isotopic composition of TN ( $\delta^{15}\text{N-TN}$ ) from 1890s to 2008.



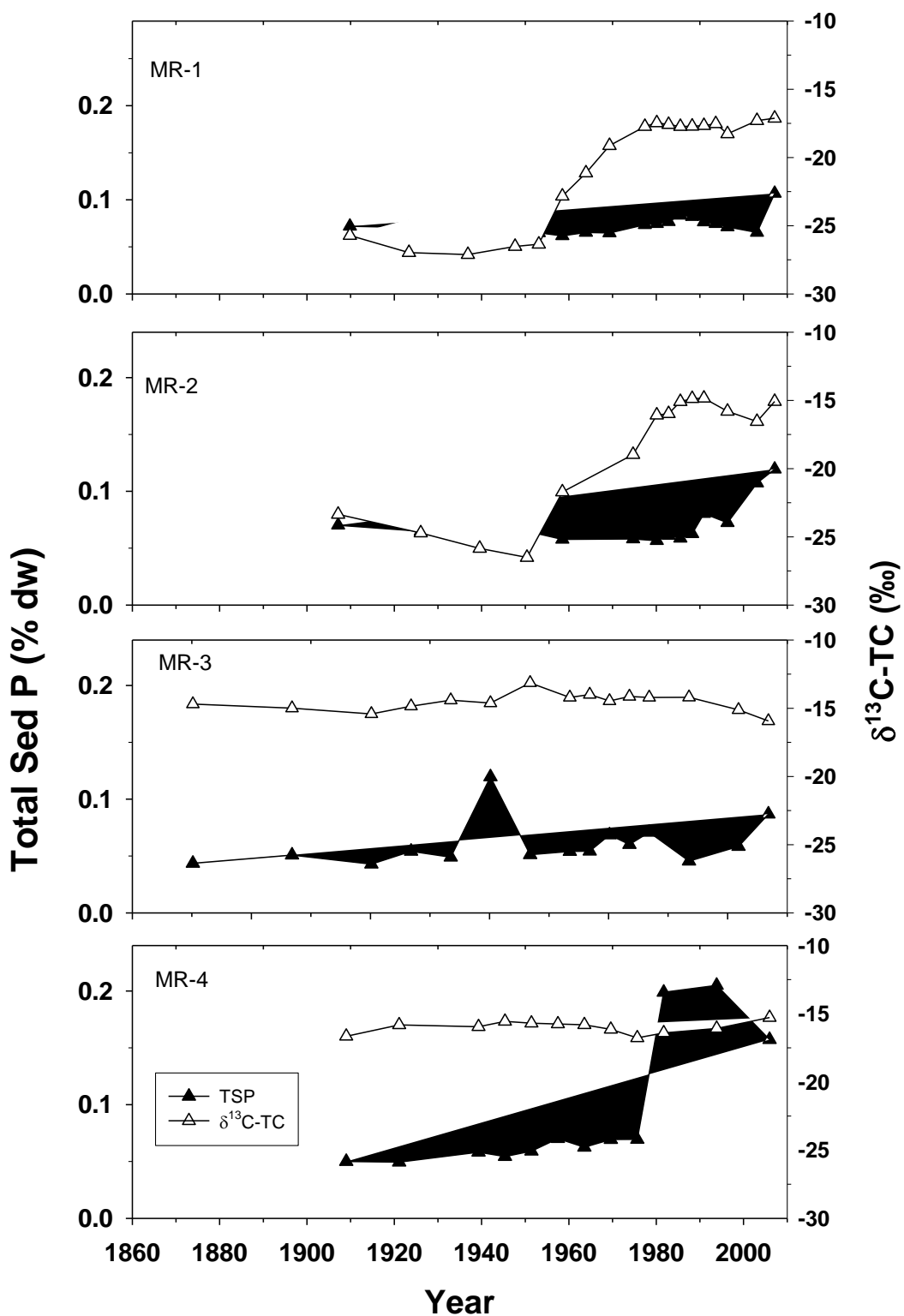


Figure 18. Concentrations of total sediment phosphorus (TSP) and the carbon isotopic composition of total carbon ( $\delta^{13}\text{C-TC}$ ) from 1890s to 2008.

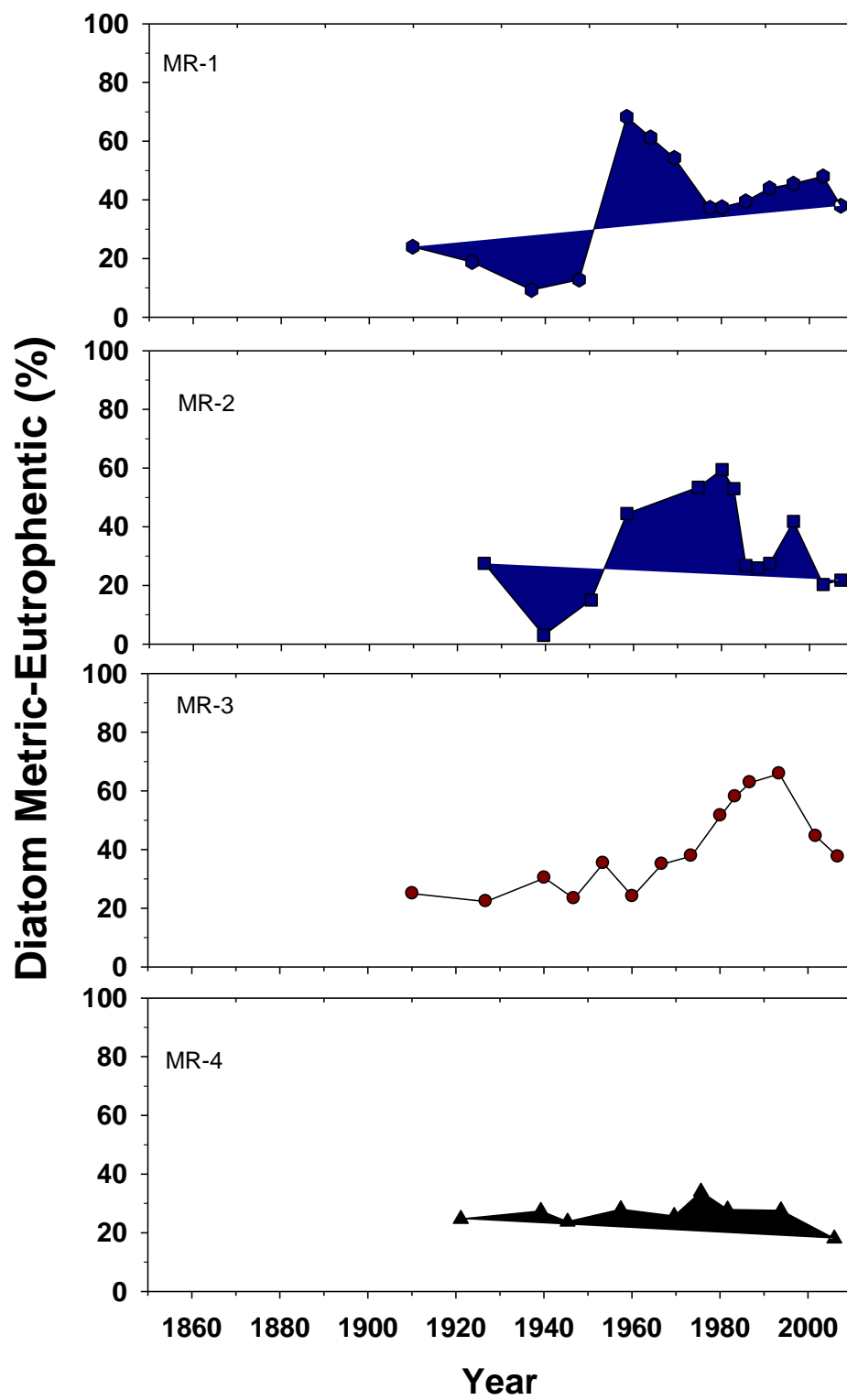


Figure 19. Diatom metric for eutrophic species from 1890s to 2003.

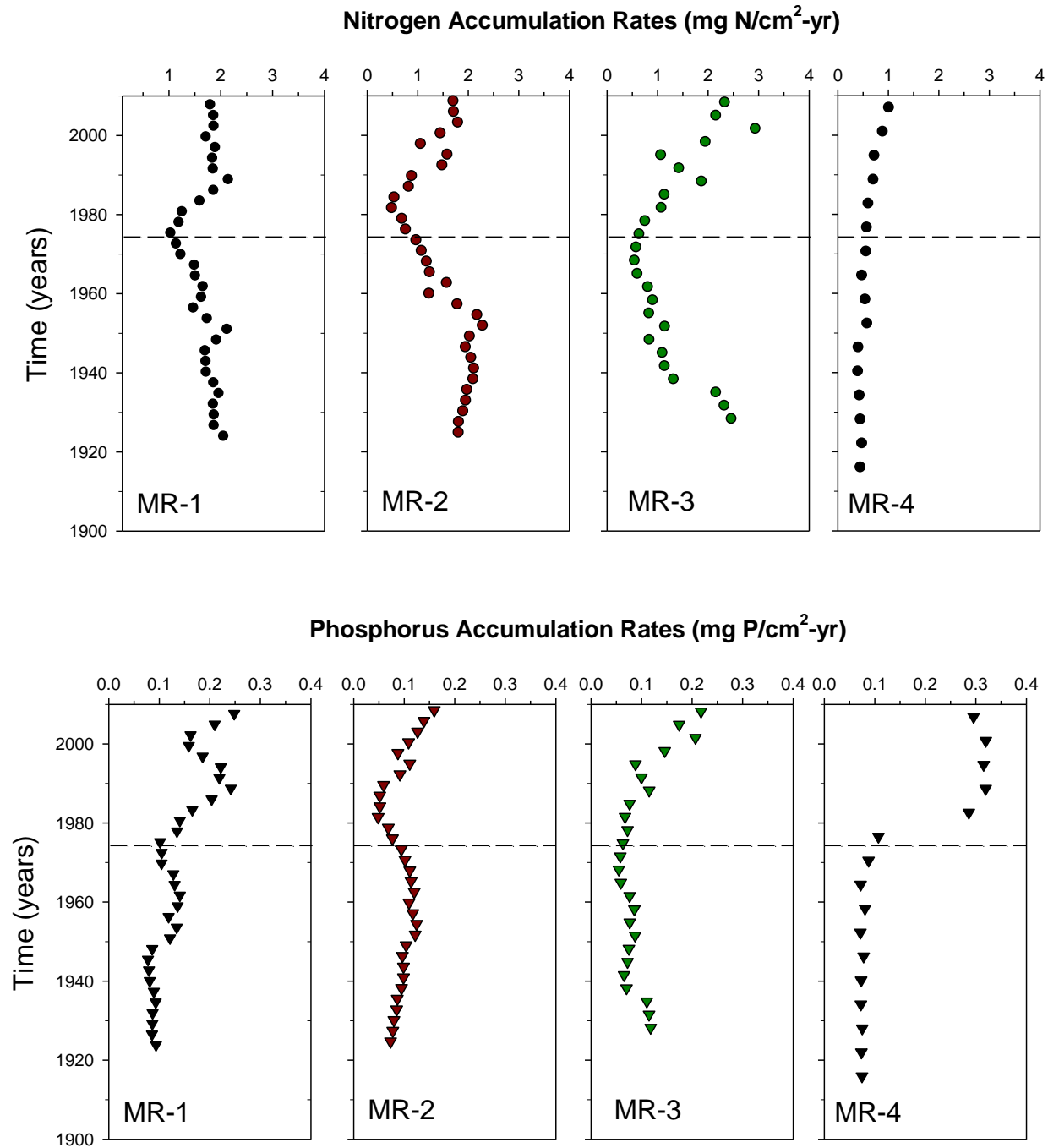


Figure 20. Nitrogen and phosphorus accumulation rates over time in tidal wetlands in the Murderkill River. Linear interpolation was used for sections of sediment that were not analyzed for N or P. The dotted line is at approximately 1975, when the KC WWTP becomes active.

## **Appendices**

Excel File with Data and QA